Nguyen *et al. Energy Mater.* **2025**, *5*, 500093
DOI: 10.20517/energymater.2024.269

Energy Materials

Review

Open Access

Recent progress on metal-organic framework-based separators for quasi-solid-state lithium metal batteries

Minh Hai Nguyen[1,#], Caofeng Niu[2,#], Nhat Minh Ngo[1], Jingwei Chen[2,3,*], Sangbaek Park[1,*]

[1]Department of Materials Science and Engineering, Chungnam National University, Daejeon 34134, Republic of Korea.
[2]School of Materials Science and Engineering, Ocean University of China, Qingdao, 266100, Shandong, China.
[3]Qingdao Key Laboratory of Marine Extreme Environment Materials, Ocean University of China, Qingdao 266100, Shandong, China.
[#]Authors contributed equally.

[*]**Correspondence to:** Prof. Jingwei Chen, School of Materials Science and Engineering, Ocean University of China, No. 238, Songling Road, Qingdao 266100, Shandong, China. E-mail: chenjingwei@ouc.edu.cn; Prof. Sangbaek Park, Department of Materials Science and Engineering, Chungnam National University, Yuseong-gu, Daejeon 34134, Republic of Korea. E-mail: sb.park@cnu.ac.kr

How to cite this article: Nguyen, M. H.; Niu, C.; Ngo, N. M.; Chen, J.; Park, S. Recent progress on metal-organic framework-based separators for quasi-solid-state lithium metal batteries. *Energy Mater.* **2025**, *5*, 500093. https://dx.doi.org/10.20517/energymater.2024.269

Received: 30 Nov 2024 **First Decision:** 6 Feb 2025 **Revised:** 23 Feb 2025 **Accepted:** 28 Feb 2025 **Published:** 27 Apr 2025

Academic Editor: Xiongwei Wu **Copy Editor:** Ping Zhang **Production Editor:** Ping Zhang

Abstract

Although lithium-ion batteries are emerging as one of the leading energy storage technologies due to their high energy density, high specific capacity, and fast charging speed, major challenges remain regarding the use of liquid electrolytes. These electrolytes directly affect the safety and durability of the batteries. While alternative materials such as rigid solid-state electrolytes have been developed to improve safety, they often suffer from poor ionic conductivity and inadequate interfacial contact with the electrodes. These issues hinder the production and widespread application of lithium-ion batteries. To overcome these disadvantages, quasi-solid-state electrolytes, which include both liquid and solid components, have been extensively researched. Among these, metal-organic frameworks (MOFs) with diverse morphological designs and porous structures are considered promising materials for the fabrication of high-performance quasi-solid-state electrolytes. This review summarizes recent research on MOF-based separators for lithium metal batteries, including native MOFs, MOF composites, and MOF derivatives. The fabrication processes and mechanisms for enhancing the electrochemical performance of each separator material are discussed. Furthermore, the prospects of this promising material for lithium metal batteries are provided.

Keywords: Quasi-solid-state electrolyte, metal-organic frameworks, Li-metal batteries, thermal stability, lithium-ion transport

INTRODUCTION

The increasing demand for high-energy-density batteries in portable electronics, electric vehicles, and grid-scale energy storage has driven the development of advanced lithium-based energy storage systems. Lithium-ion batteries (LIBs), widely used for their high energy density and long cycle life, typically rely on liquid electrolytes (LEs) due to their excellent ionic conductivity (~10^{-3} S cm^{-1})[1-4]. However, LEs suffer from inherent limitations, including high reactivity with lithium metal and cathode materials, decomposition at high voltages, and the risk of dendrite formation leading to short-circuiting and safety hazards[5-10]. These challenges have prompted significant research into alternative electrolyte systems.

The research on fabrication and application of quasi-solid-state electrolytes (QSSEs) has emerged as a promising approach, integrating the mechanical stability of solid-state electrolytes (SSEs)[11], with the high ionic conductivity of LEs. QSSEs consist of a porous solid matrix infused with a small amount of LEs, offering improved thermal stability, enhanced mechanical properties, and effective lithium dendrite suppression[12,13]. Among the various solid matrices explored, metal-organic frameworks (MOFs) have attracted significant attention due to their high porosity, tunable pore structure, and chemical versatility, making them ideal hosts for LE confinement in quasi-solid-state lithium metal batteries (QSSLMBs)[14-17].

MOFs, composed of metal nodes and organic linkers[18], provide a well-defined porous structure that facilitates efficient ion transport while maintaining mechanical robustness[19]. By tailoring MOF structures and surface functionalities, researchers have achieved enhanced ionic conductivity, uniform lithium-ion distribution, and improved interfacial stability within QSSEs[5,20,21]. Recent studies have demonstrated that MOF-based separators not only suppress lithium dendrites but also improve electrolyte retention and electrochemical stability, addressing critical challenges in QSSLMBs[15,17,22-28].

This review systematically explores the design, fabrication, and electrochemical performance of MOF-based separators in QSSLMBs. We discuss various MOF synthesis strategies, their structural characteristics, and their impact on battery performance. The review also examines MOF-based separators in different configurations, including pristine MOFs, MOF composites, and MOF derivatives. Furthermore, we highlight theoretical and experimental insights into ion transport mechanisms within MOFs and their role in mitigating common battery failure modes. Finally, we discuss challenges and future directions for the commercialization of MOF-based separators, including cost considerations, scalability, and environmental impact. By providing a comprehensive analysis of recent advancements, this review aims to guide future research on MOF-based QSSEs, facilitating the development of next-generation high-performance lithium metal batteries (LMBs).

A BRIEF INTRODUCTION OF QSSLMBS

QSSLMBs combine the high energy density of lithium metal anodes with the improved safety of QSSEs[29,30]. Unlike traditional LE-based LIBs, QSSLMBs use QSSEs that reduce leakage, flammability, and dendrite formation risks[31,32]. These electrolytes, often polymers, gels, or composites, maintain structural integrity while facilitating lithium-ion transport[29,33]. This design enhances safety, enables high electrochemical performance, and extends cycle life[1,34], making QSSLMBs promising for next-generation energy storage in applications such as electric vehicles and portable electronics[2,35].

Basic configuration

QSSLMBs consist of several key components that combine advantages of solid and LEs. The lithium metal anode provides a high theoretical capacity (3,860 mAh g^{-1}) and low electrochemical potential (-3.04 V *vs.* standard hydrogen electrode)[36,37]. The cathode, typically lithium intercalation materials (e.g., $LiNi_{1-x-y}Co_xMn_yO_2$ (NCM), $LiFePO_4$ (LFP), carbon/S)[3,38,39], enables reversible lithium-ion insertion and extraction. QSSEs, sandwiched between the anode and cathode, play a critical role in QSSLMBs, distinguishing them from all-solid-state batteries. QSSEs are typically hybrid materials, incorporating LEs within a solid framework, such as porous inorganic materials or solid organic matrices, ensuring high ionic conductivity while providing excellent thermal and mechanical stability[40,41]. The configurations of several typical QSSLMBs are illustrated in Figure 1.

The QSSE facilitates efficient ion transport while minimizing leakage, flammability, and dendrite growth risks[31,42]. The separator, usually a microporous membrane, prevents short-circuit between the anode and cathode[43]. MOF-based separators are particularly promising due to their thermal stability, tunable pore size, and high ionic conductivity[21,44-46]. Current collectors, typically copper for the anode and aluminum for the cathode, enable efficient electron transport[47].

Key design considerations for QSSLMBs include optimizing electrolyte composition for conductivity and stability[48], treating the anode surface to reduce dendrites[41], and using advanced cathode materials to enhance energy density and cycle life[1,49,50]. This integration of materials science and electrochemical engineering aims to overcome the limitations of conventional lithium-ion and solid-state batteries[51,52].

Working principle

In QSSLMBs, the QSSE is typically a solid matrix (e.g., polymers, inorganic particles, MOFs) infused with a LE, thus facilitating ion transport[13,53,54], suppressing dendrite growth[55,56], enhancing electrode contact for improved ionic conductivity[57,58], and stabilizing the solid electrolyte interface (SEI) to prevent continuous electrolyte decomposition[59,60].

During discharge, lithium ions move from the lithium metal anode through the QSSE to the cathode, while electrons flow through the external circuit[61]. During charging, lithium ions return to the anode and deposit as lithium metal[62-64]. Ion transport occurs through the liquid-filled QSSE pores, enabling electrochemical reactions and delivering power to devices[65].

The solid matrix reduces electrolyte leakage and dendrite-induced short circuits, improving battery safety, cycling stability, and lifespan[66-68]. Overall, QSSLMBs function similarly to conventional LIBs, as depicted in Figure 2, offering a balance of electrochemical efficiency and mechanical stability.

Ionic transport mechanism

Ion transport in QSSLMBs is crucial for their performance and efficiency. QSSEs typically consist of a solid matrix infused with LEs, facilitating continuous ionic pathways, reducing interfacial resistance, and promoting uniform ion distribution[31,48,69-71].

Lithium ions (Li^+) migrate through the QSSE by hopping between available sites in the solid matrix, influenced by the structural and chemical characteristics of the electrolyte material[72-76] [Figure 3A]. Incorporating MOFs into the QSSE enhances ion transport due to their high porosity, large surface area, and tunable pore structures. Functionalized MOFs lower the activation energy for ion hopping, improving mobility[77-82].

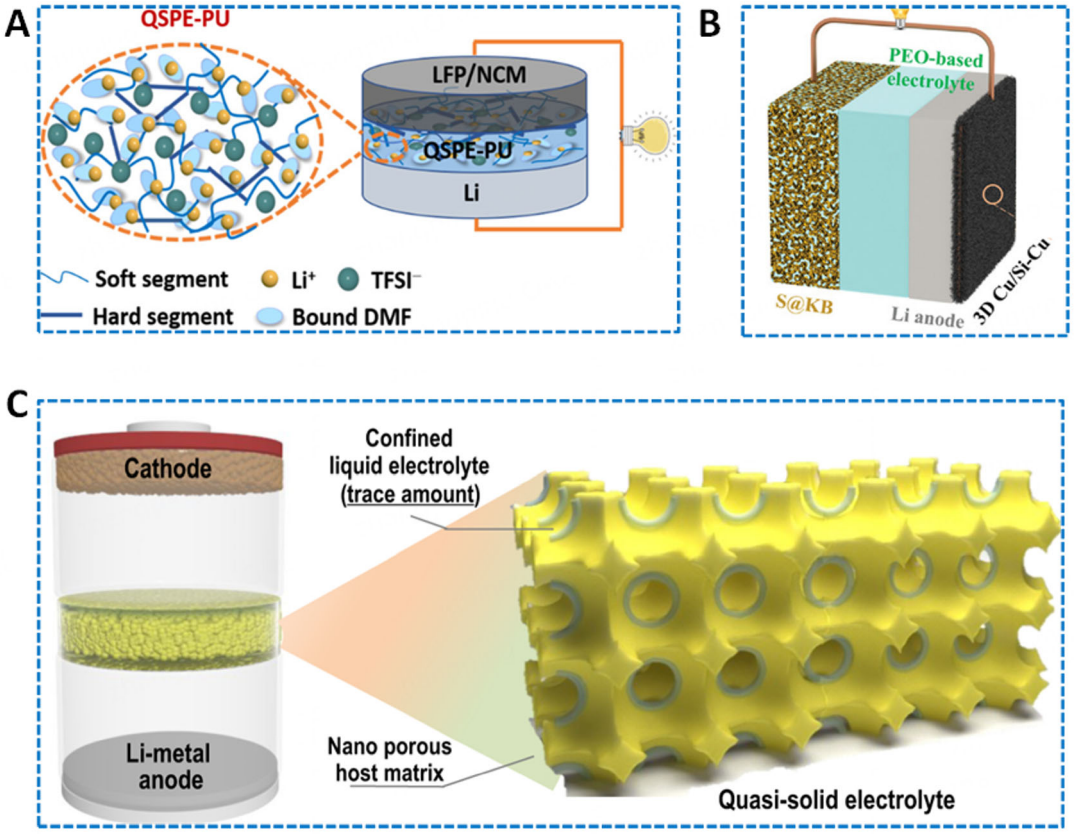

Figure 1. Schematic illustration of QSSLMBs assembled with: (A) Quasi-solid polymer electrolyte (QSPE) and NCM/LFP cathode; (B) QSPE and S cathode; (C) MOF-based QSSE and NCM/LFP cathode. (A) is quoted with permission from Fang *et al.*[49]; (B) from Wang *et al.*[50]; and (C) from Chang *et al.*[13]. QSSLMBs: Quasi-solid-state lithium metal batterie; NCM: $LiNi_{1-x-y}Co_xMn_yO_2$; LFP: $LiFePO_4$; MOF: metal-organic frameworks; QSSEs: quasi-solid-state electrolytes.

LEs in the QSSE further improve ionic conductivity by ensuring continuous ion flow and reducing interfacial resistance. This liquid phase also mitigates dendrite formation and electrolyte degradation, enhancing cycling stability [Figure 3B][13,83-86].

Ion transport in MOF-based QSSEs depends on the morphology and crystallinity of MOFs. High crystallinity and well-defined pores create continuous conduction pathways, boosting ionic conductivity[87-90] [Figure 3C]. The tunable MOF structures allow for incorporating dopants or secondary phases, improving conductivity and stability[91-93].

Electrode-electrolyte interfaces also play a critical role in ion transport. Engineering these interfaces reduces charge transfer resistance and enhances performance. In MOF-based QSSEs, modifying MOF surface chemistry or adding interfacial layers improves adhesion and ionic contact, minimizing impedance [Figure 3D][75,94-98].

Both experimental and theoretical studies provide insights into Li^+ transport in MOF-based QSSEs. Solid-state nuclear magnetic resonance (NMR) reveals complex interactions between Li^+, anions, and the MOF framework[99]. Molecular dynamics (MD) and grand canonical Monte Carlo simulations identify solvent-assisted hopping as the primary conduction mechanism in MOF-688[100,101]. MOF-688(Mn) was developed based on X-ray crystal structures, with MOF-688(Al) synthesized by substituting Mn^{3+} with Al^{3+}

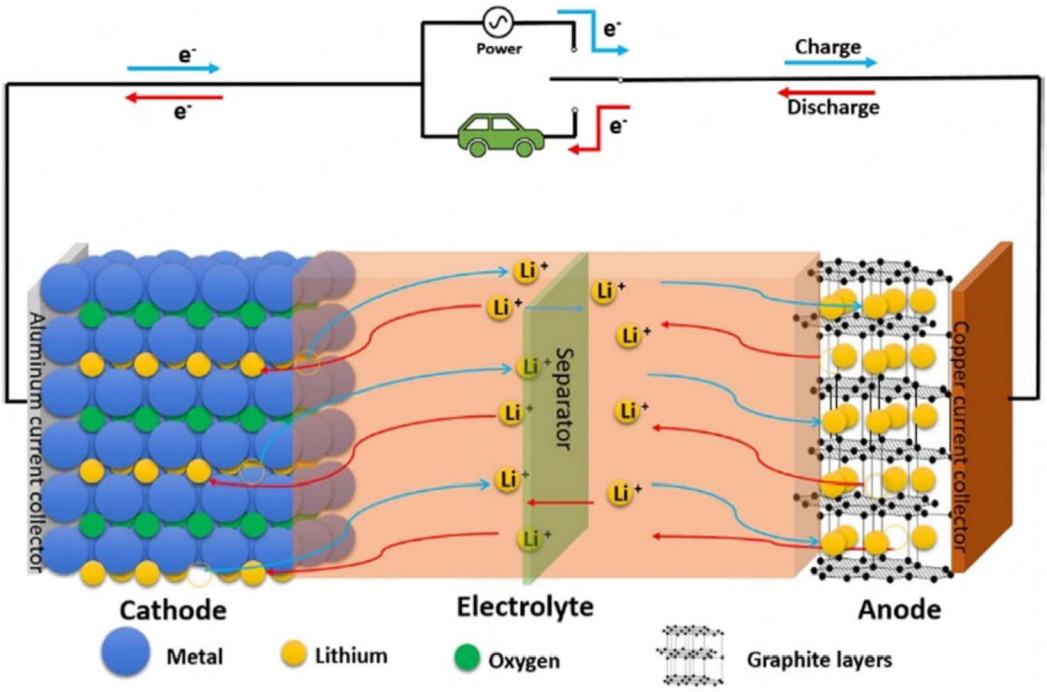

Figure 2. Schematic of the working mechanism of a gel-polymer-based lithium battery. This figure is quoted with permission from Liang *et al.*[65].

to study metal ion effects on conduction[102,103]. MD analysis identified three Li^+ motions: intra-cluster hopping, inter-cluster hopping, and bulk diffusion in propylene carbonate [Figure 3E]. Three models, Green-Kubo (GK), Nernst-Einstein (NE), and single-mechanism hopping, were used to evaluate ion conduction [Figure 3F][103]. GK measurements aligned with experimental results, confirming Li^+ hopping between polyoxometalate clusters as the dominant conduction mechanism, with minimal contribution from bulk diffusion.

In summary, ion transport in QSSLMBs involves a complex interaction of material properties, structural design, and interfacial engineering, offering enhanced ion transport through their unique structural and chemical features. The combination of experimental and theoretical approaches has advanced the understanding of ionic conduction in MOF-based QSSEs, facilitating the optimization of QSSLMBs for high-energy-density applications.

Current challenges

QSSLMBs offer a promising path to high-energy-density and safer energy storage. However, several challenges remain. A major issue is achieving high ionic conductivity in QSSEs. While LEs typically show conductivities of 10^{-3} to 10^{-2} S/cm[104,105], maintaining comparable conductivity when integrated into a solid matrix is difficult. The rigid solid matrix, often polymers, inorganic particles, or MOFs, limits ion mobility[106-108]. Ensuring uniform distribution and retention of the liquid component is also vital to prevent phase separation and leakage, which can cause performance degradation and safety risks.

Lithium dendrite formation during cycling is another key challenge, as dendrites can penetrate the separator, leading to short circuits and thermal runaway. While the solid matrix of a QSSE can inhibit dendrite growth, its effectiveness depends on the mechanical properties and material uniformity[109-111]. The QSSE must endure the mechanical stress of lithium plating and stripping while maintaining flexibility to

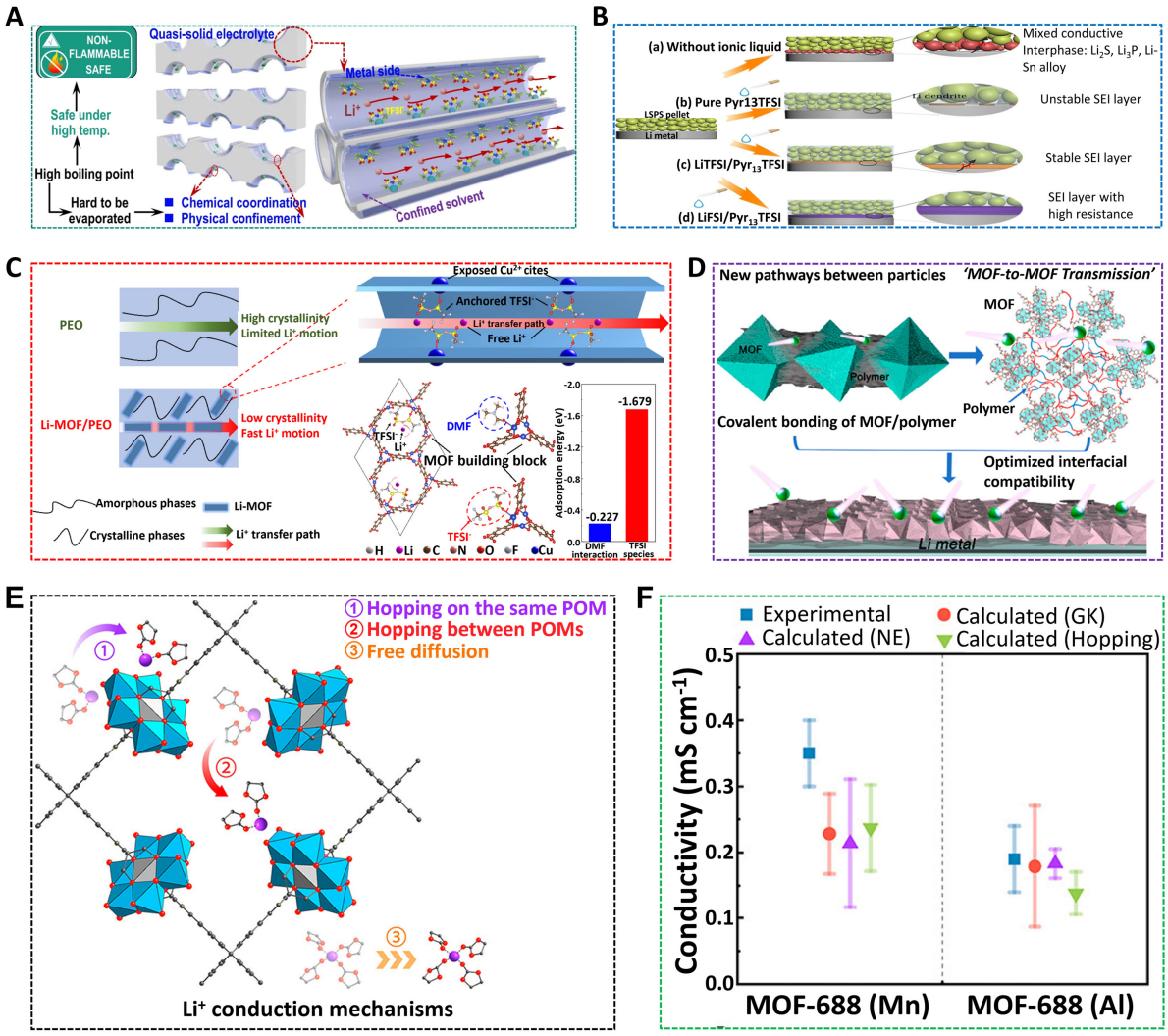

Figure 3. Schematic illustration of: (A) Li-ion transport via hopping effect in the solid-matrix channels of QSSLMBs; (B) The importance of liquid components in surface engineering of QSSE; (C) The effect of Li-MOF on lithium-ion conduction and the crystallinity of the polyethylene oxide (PEO) matrix; (D) Improvement of the adhesion and ionic contact for better Li-ion transport by modifying the surface chemistry of the MOFs; (E) Three proposed Li conduction mechanisms in MOF-based QSSEs; (F) Ionic conductivities of MOF-688(Mn) and MOF-688(Al) obtained from experimental measurements, and theoretical calculations using Green-Kubo relations (GK), Nernst-Einstein equation (NE), and simple hopping model (hopping). (A) is quoted with permission from Chang *et al.*[13]; (B) from Zheng *et al.*[86]; (C) from Zhang *et al.*[90]; (D) from Zhang *et al.*[97]; (E and F) from Hou *et al.*[103]. QSSLMBs: Quasi-solid-state lithium metal batterie; QSSEs: quasi-solid-state electrolytes; MOF: metal-organic frameworks.

accommodate volume changes during cycling. Additionally, developing QSSEs capable of forming a stable and uniform SEI is crucial for preventing electrolyte decomposition and ensuring long-term cycling stability[112,113].

Interfacial stability between the QSSE and the electrodes is another area of concern. The interfaces must facilitate efficient ion transport and prevent detrimental side reactions. While much attention has been devoted to the challenges posed by lithium metal anodes due to their high reactivity and propensity for unstable interfaces[108,114,115], the QSSE-cathode interface also presents significant challenges. Poor contact, interfacial side reactions, and the structural instability of cathode materials during cycling can lead to increased interfacial resistance and capacity degradation[116-118]. Strategies such as surface coatings, functional

interlayers, and MOF modifications can improve interfacial compatibility and reduce resistance at both electrode interfaces. However, these approaches introduce complexities and potential new failure modes that must be carefully addressed.

The fabrication and scalability of QSSEs with consistent and reproducible properties also present significant challenges. The synthesis of MOFs with desired porosity and chemical functionality requires precise control over the conditions, and scaling up these processes for industrial production can be complex and costly[33,110,119-121] [Figure 4]. While Ni-based MOFs have been widely explored, other metal precursors, such as Zn, Zr, and Cu, offer alternative design possibilities, each with distinct cost implications. For instance, Zr-based MOFs tend to have higher raw material costs due to the expense of zirconium precursors, whereas Zn and Cu-based MOFs may provide cost advantages in large-scale production[122,123]. Furthermore, the choice of organic ligands, such as terephthalic acid, imidazolates, and carboxylates, can significantly influence the overall material cost and process efficiency[123,124]. Additionally, integrating MOFs into composite electrolytes must ensure uniform dispersion of the liquid component to maintain high ionic conductivity and mechanical stability. The cost and environmental impact of these advanced materials are further considerations, as MOFs and other solid matrix components often involve expensive and energy-intensive synthesis methods[33,40].

Thermal stability and chemical compatibility of QSSEs with the lithium metal anode and high-voltage cathodes are crucial for safe battery operation. The QSSE must endure high temperatures and reactive environments without degrading. While MOFs offer good thermal stability, they must be carefully selected and modified to prevent degradation under operational conditions[108,113]. Additionally, the QSSE must prevent side reactions with high-voltage cathodes to maintain performance and safety over extended cycles[51].

The long-term cycling stability and reliability of QSSLMBs also require extensive validation under real-world conditions. While laboratory tests show promise, practical applications demand rigorous testing for capacity retention, rate capability, and safety under various abuse conditions. QSSEs must sustain performance and safety over thousands of cycles to enable commercialization[114,125-127].

In conclusion, while QSSLMBs offer a promising route to safer and more efficient energy storage, addressing challenges in optimizing ionic conductivity, preventing dendrite formation, ensuring interfacial stability, achieving scalable fabrication, and maintaining thermal and chemical stability is essential. Continued research, particularly leveraging unique properties of MOFs, will be key to advancing QSSLMBs for practical use.

General strategies for designing QSSEs

Designing QSSEs for LMBs involves integrating innovative strategies to enhance ionic conductivity, mechanical stability, and electrochemical performance. One approach is incorporating a LE or ionic liquid into a solid inorganic electrolyte matrix, combining high ionic conductivity of the LE with structural stability of the solid matrix [Figure 5A][128]. For instance, Zhang *et al.* improved ion transport and suppressed dendrite formation by integrating a TFSI [bis(trifluoromethanesulfonyl)imide]-based ionic liquid into a garnet-like $Li_7La_3Zr_2O_{12}$ (LLZO) framework, achieving a stable and conductive QSSE[129].

MOF-based QSSEs leverage the high surface area, tunable porosity, and chemical versatility of MOFs [Figure 5B][130]. For example, Subramani *et al.*[131] incorporated Fe-MIL-101 into a poly(vinylidene fluoride-co-hexafluoro propylene) (PVdF-HFP) quasi-solid polymer electrolyte (QSPE), enhancing ionic

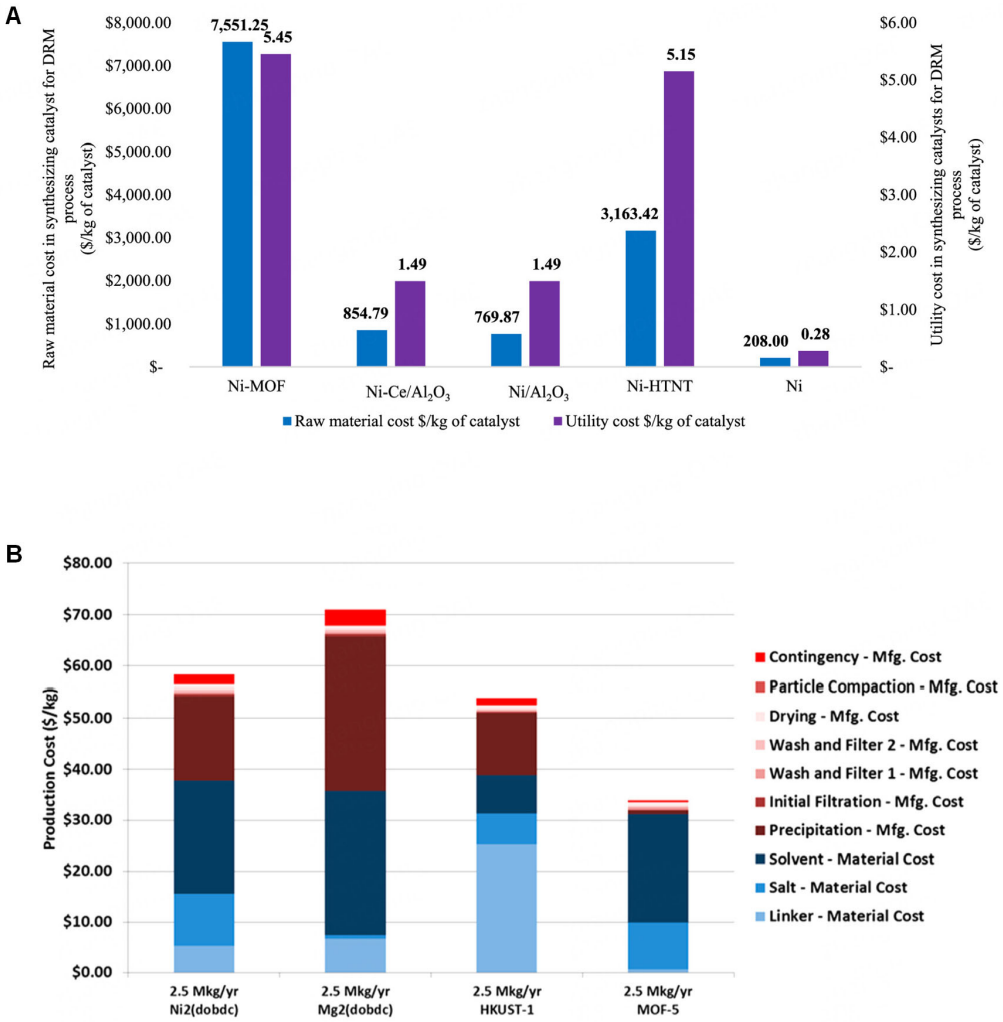

Figure 4. (A) Raw material cost and utility cost required for Ni-based MOF's synthesis; (B) Material cost contributions (linker, metal salts, and solvents) of four MOFs manufactured at 2.5 million kg/year by solvothermal synthesis methods. (A) is quoted with permission from Ong *et al.*[120]; (B) from DeSantis *et al.*[121]. MOF: Metal-organic frameworks.

conductivity and mechanical stability. The porous structure of MIL-101 facilitates continuous ion pathways, improving battery efficiency.

QSPEs are a specific subclass of QSSEs that utilize a polymer matrix, such as polyethylene oxide (PEO) or polyvinylidene fluoride (PVDF), swollen with a LE to enhance ion mobility while maintaining mechanical support. Unlike MOF-based or inorganic-supported QSSEs, QSPEs primarily rely on the polymer structure for mechanical integrity. Homann *et al.*[132] developed QSPE using LiTFSI incorporating PEO polymer matrix, achieving high ionic conductivity and excellent electrochemical stability [Figure 5C]. The interconnected network of the polymer matrix facilitates ion transport, maintains flexibility, and enhances compatibility with lithium metal electrodes.

Inorganic-polymer composite electrolytes combine the high ionic conductivity of inorganic materials with the mechanical flexibility of polymers [Figure 5D]. Wang *et al.* developed a composite electrolyte using lithium aluminum titanium phosphate (LATP) embedded in a polytetrafluoroethylene (PTFE) matrix,

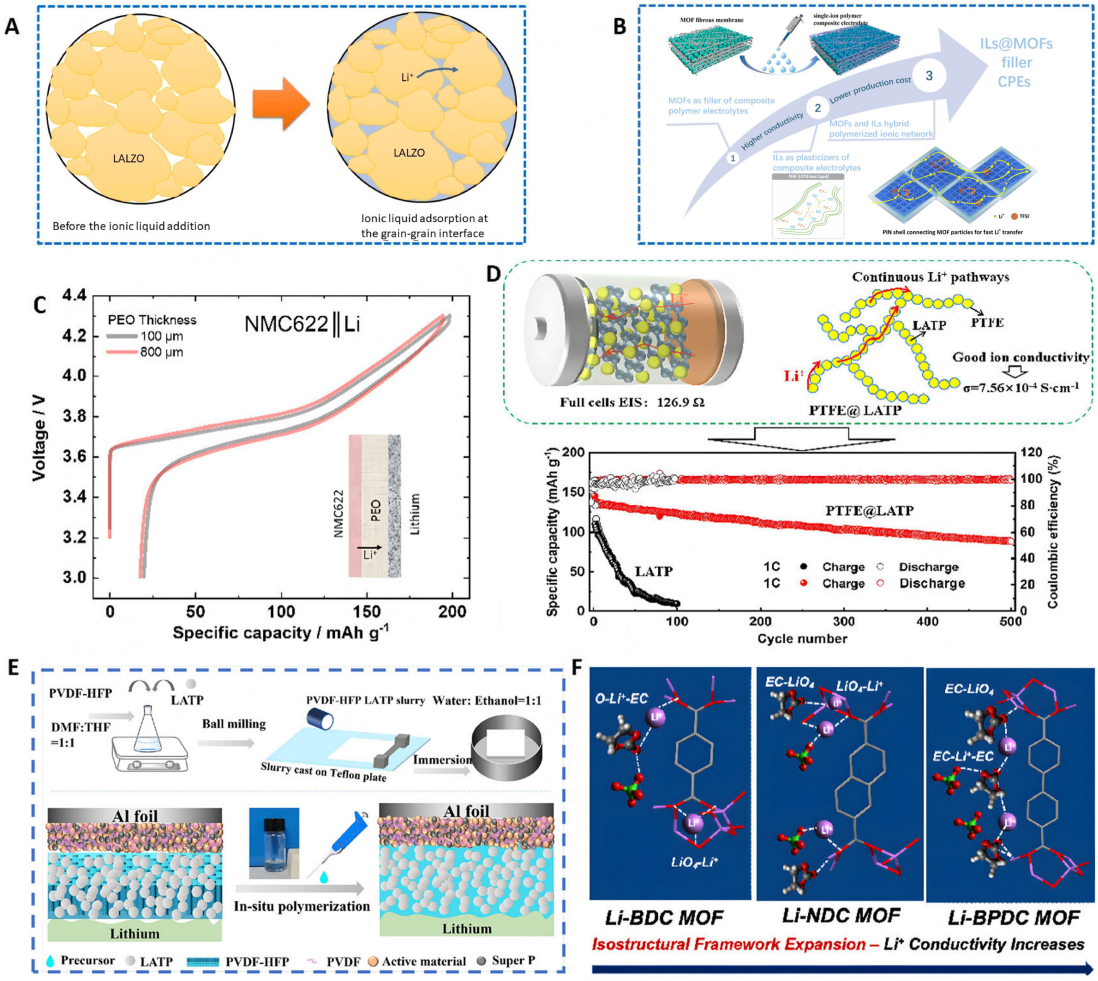

Figure 5. (A) Integrating TFSI-based ionic liquid into a garnet-like $Li_{6.75}Al_{0.25}La_3Zr_2O_{12}$ (LALZO) framework for better ion transport and suppression of lithium dendrite formation; (B) The development of MOF-based QSSEs; (C) PEO-based QSSE for high-performance NMC622//Li batteries; (D) Constructing PTFE@LATP composite solid electrolytes with three-dimensional network for high-performance lithium batteries; (E) Schematic illustration of the porous LATP-PVDF-HFP membrane preparation process and the *in-situ* polymerization; (F) Isostructural Li-MOF expansion for high ionic conductive QSSE. (A) is quoted with permission from Kaur *et al.*[128]; (B) from Lin *et al.*[130]; (C) from Homann *et al.*[132]; (D) from Wang *et al.*[133]; (E) from Liu *et al.*[134]; and (F) from Butreddy *et al.*[136]. MOF: Metal-organic frameworks; QSSEs: quasi-solid-state electrolytes; PEO: polyethylene oxide; PTFE: polytetrafluoroethylene; LATP: lithium aluminum titanium phosphate; TFSI: trifluoromethylsulfonyl; PVDF: polyvinylidene fluoride; HFP: hexafluoro propylene.

enhancing both ion conduction and mechanical strength[133].

In situ polymerization is another advanced strategy where MOFs or inorganic particles are uniformly dispersed within the polymer matrix during polymerization [Figure 5E][134]. Xu *et al.* used Li^+-containing liquid monomers with a MOF-incorporated fibrous membrane for *in situ* polymerization, achieving superior stability and enhanced ion transport[135].

Intrinsically, lithium-ion conductive MOFs represent another promising development. These MOFs integrate lithium ions directly within their framework, ensuring stable ion conductivity. Butreddy *et al.* demonstrated a lithium-based MOF with both structural stability and high ionic conductivity, improving QSSE performance in LMBs[136] [Figure 5F].

Other strategies include cross-linking polymer networks to enhance dimensional stability during cycling[137-140], using nanocomposites with carbon-based materials like graphene or carbon nanotubes to improve mechanical and electrochemical properties[141], and employing electrospinning techniques to fabricate QSSEs with aligned nanofiber structures for better ion transport and mechanical performance[142].

In summary, QSSE design involves approaches such as integrating LEs into solid matrices, utilizing MOF-based materials, and developing polymer-inorganic composites. These strategies aim to optimize ionic conductivity, mechanical stability, and electrochemical performance, advancing toward safer and more efficient LMBs.

PREPARATION OF MOF-BASED QSSES

Different LMBs often encounter inherent problems including shuttle effect and dendrite growth during operation[143-145]. Shuttle effect results in decreased capacity and poor cycling stability[146], while heterogeneity in surface morphology, concentration gradient and uneven electrical field distribution on the anode can often cause deposition of metal protuberances that evolve into dendrites[147]. To address these issues, separator design is an effective strategy via regulating ion fluxes and electric field distribution[148]. MOFs have abundant micro/mesopores with tunable sizes, regular structures [Figure 6A], and ample active sites [Figure 6B][149]. Incorporating MOFs into separators is an effective strategy to promote the cycling stability of batteries via catalyzing polyanion conversion, inhibiting shuttle effect, and homogenizing electric/concentration field distribution[150,151]. MOFs with abundant active sites can effectively promote cation transfer, prevent the diffusion of by-products, and ensure a uniform electrical field, thereby inhibiting the notorious shuttle effect and dendrite growth [Figure 6B-D][152-154]. In this section, the effect of MOF synthesis parameters, separator preparation methods, and MOF activation on the performance of MOF-based separators/QSSEs, will be thoroughly discussed.

Synthesis of MOFs

MOFs have intriguing properties for various applications, including gas storage and separation[155,156], chemical catalysis[157], sensing[158], ion exchange[159], drug delivery[160], and electrolyte fillers. MOFs are often categorized into MOFs (isoreticular MOFs), zeolite-imidazolate frameworks (ZIFs), materials of Institute Lavoisier (MILs), pocket-channel frameworks (PCNs) and other series based on the structure or named after the institution firstly reporting the synthesis. This section will discuss the application of MOFs in battery separators, mostly centered on Zr-, Zn-, Cu-, and other metal ion-based MOFs.

Zr-based MOF

UIO-66 {$[Zr_6O_4(OH)_4][1,4\text{-benzene dicarboxylate (BDC)}]_6$} is a typical Zirconium-based MOF and one of the most representative MOFs[161], which can be used as a nano-filler in QSSEs and can be obtained via various synthesis methods[162], yet solution-process are more commonly used to obtain different Zr-based MOFs by changing the organic linkers. Lei[144] *et al.* prepared UIO-66 through hydrothermal method with $ZrCl_4$ and BDC in N, N-dimethylformamide (DMF) [Figure 6E]. The as-obtained UIO-66 was added to the QSSE of Al-Se batteries to improve battery performance. Notably, tuning metal ions to ligands ratio greatly affects the structure and properties of the obtained MOFs. For example, the total N_2 absorption of UIO-66 synthesized using metal ions to ligand ratios of 6:6, 6:4, and 6:3 were 12.9 mmol g^{-1}, 12.2 mmol g^{-1}, and 13.3 mmol g^{-1}, respectively, at 0.97 P/P_0[163]. MOFs having more pores with wider size distribution will have more contact and interaction with the electrolyte, increasing the proton concentration inside the pores, thereby strengthening the Coulomb interaction between the charge carrier and the pore surface and improving conductivity[164]. In addition, the presence of water in the raw material can also affect the crystallinity of the as-obtained MOFs. Crystalline UIO-66 can only be obtained with appropriate amount of

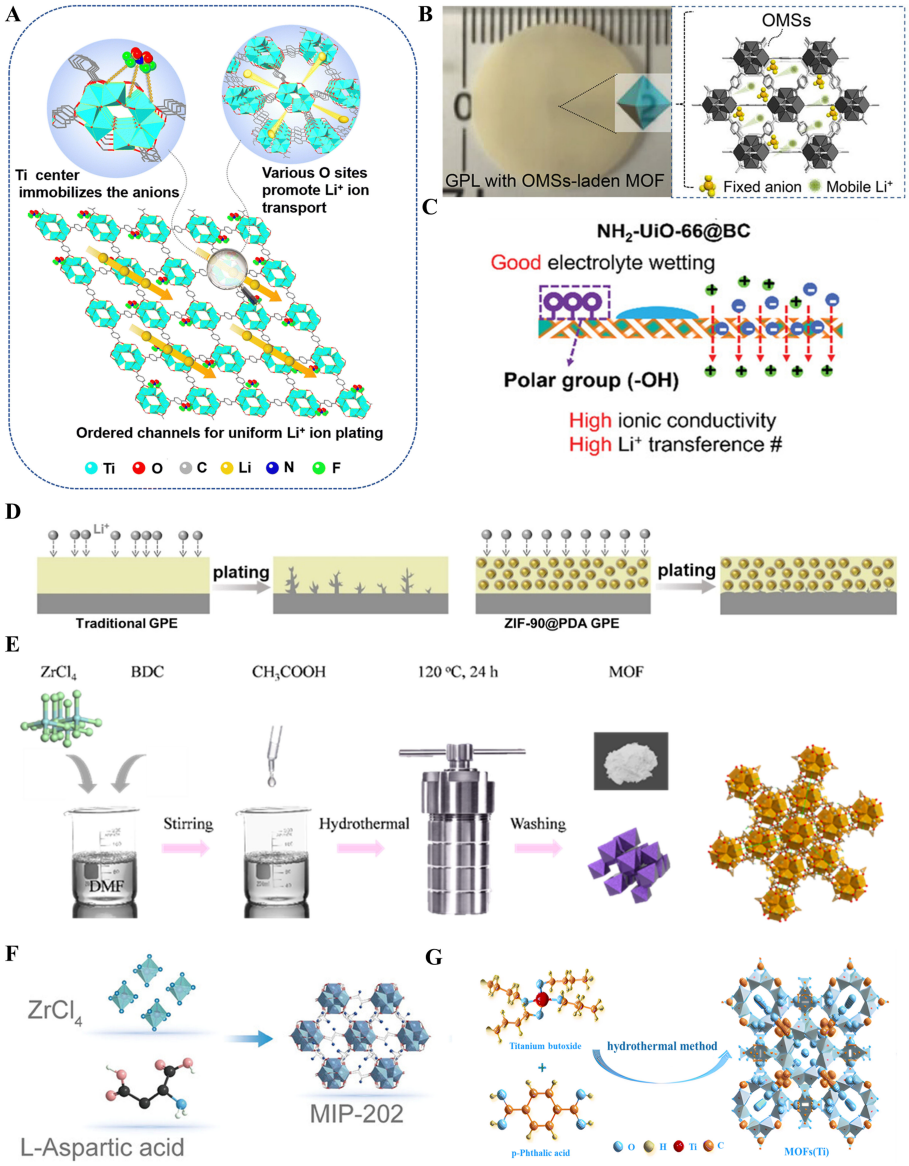

Figure 6. (A) A typical MOF structure, where metal ions and organic ligands form a regular two-dimensional framework; (B) Rich active sites on MOFs; (C) MOF modified separators regulate the electric field and guide the ion flux; (D) MOF modified separator guides the uniform metal deposition and avoids dendrite formation; Representative synthesis process of (E) UIO-66; (F) MIP-202 and (G) MIL-125 (Ti). (A and G) are quoted with permission from Liu *et al.*[149]; (B) from Lu *et al.*[152]; (C) from Fu *et al.*[153]; (D) from Wang *et al.*[154]; (E) from Lei *et al.*[144]; and (F) from Zhou *et al.*[166]. MOF: Metal-organic frameworks.

water, insufficient or excess water will render amorphous UIO-66 or other by-products. Aside from UIO-66, other Zr-based MOFs are also available. UIO-67 can be obtained by gradually adding solution A [biphenyl-4,4'-dicarboxylicacid (BPDC) and triethylamine in DMF] to solution B ($ZrCl_4$ and acetic acid in DMF) for subsequent hydrothermal reaction[165]. MIP-202(Zr) can be obtained by refluxing $ZrCl_4$ and L-aspartic acid in aqueous solution [Figure 6F][166]. Nonetheless, there are some Zr-based MOFs that have not yet been applied to QSSEs, such as PCN[167] series and MOF-808. PCN-221 can be obtained by heating $ZrCl_4$ mixed with [Tetrakis (4-carboxyphenyl)porphyrin] (TCPP), acetic acid, and N, N-diethylformamide (DEF). PCN-222 is synthesized by mixing $ZrOCl_2 \cdot 8H_2O$, TCPP, DEF, 4-tert-butylbenzoic acid and heating. PCN-223 can be synthesized by heating a mixture of $ZrOCl_2 8H_2O$, TCPP, 4-chlorobenzoic acid, formic acid,

and DMF. PCN-224 is synthesized by heating a mixture of $ZrCl_4$, TCPP, benzoic acid, and DMF. Among them, the formation of PCN-224 takes a longer holding time of 24 h at 120 °C, while the other three require 12 h under the same temperature. Furukawa[168] *et al.* synthesized MOF-808 with a structure similar to UIO-66 by hydrothermal treatment of H_3BTC (1,3,5-Benzenetricarboxylic acid) and $ZrOCl_2 \cdot 8H_2O$ in a mixed solvent of formic acid and DMF. Other MOF-80-series, for example MOF-802, MOF-805, and MOF-806 can also be obtained by just replacing H_3BTC with 1H-pyrazole-3,5-dicarboxylic acid (H_2PZDC), 1,5-Dihydroxynaphthalene-2,6-dicarboxylic acid [$H_2NDC-(OH)_2$], and 3,3'-dihydroxy-4,4'-biphenyldicarboxylic acid [$H_2BPDC-(OH)_2$], respectively.

Zn-based MOF

The majority of MOFs in the ZIF series are Zn-based MOFs, with a small portion being Co-based MOFs. Zn-based MOFs commonly used in separators/QSSEs include ZIF-8, ZIF-69, and ZIF-90. ZIF-8 and ZIF-69 can be prepared at room temperature. For example, ZIF-8 is obtained by a simple one-step copolymerization of Zn (II) and 2-methylimidazole in methanol[169], and ZIF-69 can be fabricated via mixing aqueous solutions of zinc nitrate hexahydrate, 2-nitroimidazole (HNIM) and 5-chlorobenzimidazole (H-ClBIM)[170]. ZIF-90 can be synthesized in both DMF or deionized water[171], but room temperature synthesis in aqueous/alcohol solvent is more favorable because the particle size of ZIF-90 synthesized by solvothermal in DMF is often too large. Mixing solutions of zinc nitrate in water/alcohol (ethanol, 2-propanol, iso-butanol, and tert-butanol) and iminazole-2-carboxaldehide (ICA) and polyvinylpyrrolidone (PVP) in water can obtain ZIF-90. Aside from temperature/solvent, molar ratios of raw materials also affect the particle size of ZIF-8/ZIF-90[172]. When the Hmim/Zn molar ratio is 40 and 100, the average crystal sizes of ZIF-8 are 2 mm and 250 nm, respectively. Similarly, when the ratio of ICA/Zn changed from 4:1 to 60:1, the particle size of the synthesized ZIF-90 decreased from approximately 2,500 nm to 450 nm. Obviously, increasing the ratio of Zn/ligand ratio renders ZIF-90 with larger sizes and ZIF-8 with smaller sizes. Using $Zn(NO_3)_2$ as the metal ion source while changing the organic ligand and solvent, other Zn-MOFs can be synthesized. For example, heating $Zn(NO_3)_2$ mixed with imidazole in DMF can yield ZIF-6 and ZIF-10[173]. Mixing $Zn(NO_3)_2$ with purine and DEF can synthesize ZIF-20[174]. In addition to the ZIF series, other Zn-based MOFs including MOF-2 and MOF-5 also deserve attention. The synthesis of both MOF-2 and MOF-5 involves $Zn(NO_3)_2$, DMF, and 1,4-benzenedicarboxylic acid (H_2BDC), while heating at 95 °C renders MOF-2 with a square lattice and heating at 120 °C renders MOF-5 with a cubic lattice[175].

Cu-based MOF

Cu-based MOF is another type of commonly used MOF for battery separators. Cu-TCPP nanosheets can be obtained by solvothermal reaction of $Cu(NO_3)_2 \cdot 3H_2O$ and 5, 10, 15, 20-tetrakis (4-carboxyphenyl) porphyrin (H_2TCPP) in a mixture of DEF and ethanol[176,177], whereby HKUST-1 can be obtained via room temperature mixing of $Cu(NO_3)_2 \cdot 3H_2O$/PVP-K30 and H_3BTC in anhydrous methanol. Reducing PVP molecular weight can transform HKUST-1 from microparticles into nanoparticles. Likewise, monitoring the feeding rate of raw materials can also control the nucleation process, preparing HKUST-1 with a size distribution in the range of 89~503 nm[178]. Additionally, adjusting the amount of template reagent cetyltrimethylammonium bromide (CTAB) during microwave-assisted synthesis resulted in HKUST-1 with graded porous defects, and thus size gradient micropores[179].

Aside from Cu-TCPP and HKUST-1, other Cu-based MOFs [e.g., coordination pillared-layer (CPL) series and Dresden University of Technology (DUT) series] are also available but not yet used as nanofillers for batteries. CPL-1 can be obtained by adding NaOH dropwise to a mixed solution of $Cu(NO_3)_2 \cdot 3H_2O$, pyz (Pyrazine), H_2PZDC, and H_2O under stirring, and then heating for 12 h[180]. CPL-2 can be synthesized by uniformly mixing H_2PZDC with NaOH aqueous solution and ethanol, and slowly adding it to

$Cu(ClO_4)_26H_2O$ aqueous solution with stirring[181]. As reported by Garai *et al.*[182], the Cu ions within DUT-49 can be replaced with other metal ions via ion exchange. The diversity of its types and inherent flexibility render the DUT series as potential electrolyte fillers. DUT-49 can be obtained by mixing $Cu(NO_3)_23H_2O$ with DMF and heating for 13 days, and subsequent addition of acetic acid. Similarly, by changing the ratio of raw materials, DUT-46, DUT48, and DUT-50 can be synthesized using the same method[183].

MOFs based on other metals

Aside from Zr-, Zn- and Cu-based MOFs, other metal-based MOFs, including Cr-, Mg, Ti- and Al-, also deserve attention. MIL-100(Cr) can be synthesized by heating the grinded $CrCl_3·6H_2O$ and H_3BTC precursor with deionized water vapor in a layered hydrothermal reactor using steam assisted method[184]. MIL-101(Cr) was synthesized by hydrothermal synthesis by mixing H_2BDC with $CrCl_3·6H_2O$ in deionized water[185]. Dissolving $Mg(CH_3COO)_2$ and 2,5-dihydroxytryphthalic acid (H_4dhtp) in a mixed solvent of DMF/ethanol/water can render Mg-MOF-74. Notably, Hu *et al.*[186] found that increasing the reaction time can cause the aggregation of Mg-MOF-74 nanorod seeds into well-crystallized bulk crystals with decreased grain size. The synthesis of MIL-125(Ti) is dependent on a solvothermal method[187], which can be done by quickly adding tetrabutyl titanate $Ti(OC_4H_9)_4$ to H_2BDC in DMF/anhydrous methanol, stirring and subsequent solvothermal reactions [Figure 6G]. Al-based MOF-303 can be prepared by slowly dissolving $AlCl_3·6H_2O$ in a mixed aqueous solution of NaOH and 3,5-pyrazolecarbolic acid under ultrasonic treatment, and subsequent heating[188].

Clearly, the porosity and grain size of MOFs can be regulated by many factors, such as tuning the ratio of metal ion to organic ligand[189], reaction temperature, nucleation process, *etc.*, influence the proton conductivity, electronic conductivity, and Lewis acid sites of the as-obtained MOFs. However, the effect of synthesis factors on different MOFs might vary, as has been discussed for the effect of metal/ligand ratio on the grain sizes of ZIF-8 and ZIF-90. Therefore, attention should be paid to the influence of various parameters when synthesizing MOFs, so as to prepare MOFs with desirable properties. In Table 1, the raw materials, topological structure, pore size, and other parameters of MOFs mentioned in this section are summarized.

Fabrication of MOF-based separators

MOF-based separators are often obtained by grafting MOFs onto different substrates (e.g., commercial polypropylene (PP) and electrospun separators) or dispersing MOFs into different matrices. In the meantime, different surface modification strategies of MOFs are also employed to improve the electrochemical performance of MOF-based separators in different batteries. In this section, several preparation methods for MOF-based separators (including QSSEs) will be introduced.

Scrape coating

One of the most straightforward way to graft MOFs onto different substrate is scrape-coating. Leng *et al.*[190] dispersed Ni-Co MOF, graphene and PVDF in n-methyl-2-pyrrolidone (NMP), and the slurry can be subsequently scrape-coated onto a commercial PP separator (PPS). Similarly, Razaq *et al.*[191] mixed ZIF-8, Super-P, and PVDF in NMP to prepare a slurry via ball milling, the obtained slurry was then scrape-coated onto Celgard 2400 to obtain ZIF-8 based separators. Wang *et al.*[154] prepared QSSEs using polydopamine (PDA)-modified ZIF-90 via scrape-coating assisted fabrication [Figure 7A]. ZIF-90 and PVDF-HFP were dispersed in NMP using a homogenizer; the slurry was then scrape-coated onto the electrode/glass plate. Finally, ZIF-90 modified QSSE can be obtained by injecting the ionic LE (ILE) into the scrape-coated support layer for subsequent heating, where the ILE contains 1M LiTFSI dissolved in

Table 1. Synthetic materials and characteristics of common MOFs

MOFs	Metal ion source	Organic ligand	Solvent	Structure	Micro-pore size (Å)	Surface area S_{BET} (m^2/g)	Reference
UIO-66	$ZrCl_4$	BDC	DMF	Multi-level pore structure	Tetrahedral cages: 8 Octahedral cages: 11	1,000-1,500	[162]
UIO-67	$ZrCl_4/ZrCl_2 \cdot 8H_2O$	BPDC	DMF+CH_3COOH	Multi-level pore structure	Tetrahedral cages: 12 Octahedral cages: 16	1,500-2,000	[165]
MIP-202(Zr)	$ZrCl_4$	L-aspartic	H_2O	Octahedral microporous structure	Octahedral cages: 6.3	49.62	[166]
PCN-221	$ZrCl_4$	TCPP	DEF+CH_3COOH	Directional disordered $Zr_6O_4(OH)_4$ clusters	Cube cage 19	463	[167]
PCN-222	$ZrCl_2 \cdot 8H_2O$	TCPP	DEF+ 4-tert-butylbenzoic acid	Cube 3D porphyrin framework	11	2,169	[167]
PCN-223	$ZrCl_2 \cdot 8H_2O$	TCPP	4-chlorobenzoic acid+HCOOH	SHP-a topology structure	11	617	[167]
PCN-224	$ZrCl_4$	TCPP	DMF+ benzoic acid	SHP topology structure	19	1,334	[167]
MOF-808	$ZrCl_2 \cdot 8H_2O$	H_3BTC	DMF+HCOOH	SPN topology structure	Tetrahedral cages:4.8	1,300-1,700	[168]
ZIF-6	$Zn(NO_3)_2$	Imidazole	DMF	GLS-type silicon aluminum molecular sieve network	8.8	-	[173]
ZIF-8	$Zn(NO_3)_2$	2-methylimidazole	CH_3OH	SOD type silicon aluminum molecular sieve network	4.31	1,187-1,836	[169]
ZIF-20	$Zn(NO_3)_2$	purine	DEF	RHO-type silicon aluminum molecular sieve network	14.64	-	[174]
ZIF-69	$(CH3COO)_2$ Zn	2-nitroimidazole+ 5-Chlorobenzimidazole	CH_3OH	GME topology structure	7.8	1,070	[170]
ZIF-90	$Zn(NO_3)_2$	ICA+PVP	H_2O+ mixed alcohols (ethanol, 2-propanol, iso-butanol, and tert-butanol)	SOD-type silicon aluminum molecular sieve network	3.4	1,000-1,500	[171]
MOF-2	$Zn(NO_3)_2$	H_2BDC	-	2D-Micro porous network	-	310	[175]
MOF-5	$Zn(NO_3)_2$	H_2BDC	-	Cubic lattice structure	15	2,900	[175]
CuTCPP	$Cu(NO_3)_2 \cdot 3H_2O$	H_2TCPP	DEF+CH_3CH_2OH	2D nanosheet	10	321.92	[176]
HKUST-1	$Cu(NO_3)_2 \cdot 3H_2O$	H_3BTC	CH_3OH	TBO type topological structure	Cube cages:11 Octahedral cages:5	1,200-1,500	[178]
CPL-1	$Cu(NO_3)_2 \cdot 3H_2O$	Pyrazine+ H_2PZDC	NaOH aqueous solution	Pillared-layer framework	10-13	330-490	[180]
CPL-2	$Cu(ClO_4)_2.6H_2O$	H_2PZDC	NaOH aqueous solution	Pillared-layer framework	6 × 8	490-546	[181]
DUT-48	$Cu(NO_3)_2 \cdot 3H_2O$	-	DMF+ CH_3COOH	Cubic octahedral supramolecular 3D framework	Octahedral cages 18.7 Tetrahedral cages 14.8 Cuboctahedral cages 10.7	4,560	[183]
DUT-49	$Cu(NO_3)_2 \cdot 3H_2O$	-	DMF+ CH_3COOH	Cubic octahedral supramolecular 3D framework	Octahedral cages 24.8 Tetrahedral cages 17.6	5,476	[183]

					Cuboctahedral cages 10.5		
DUT-50	$Cu(NO_3)_2·3H_2O$	-	DMF+ CH_3COOH	Cubic octahedral supramolecular 3D framework	Octahedral cages 30.7 Tetrahedral cages 21 cuboctahedral cages 10.7	5,476	[183]
MIL-100(Cr)	$CrCl_3·6H_2O$	H_3BTC	-	MTN zeolite topology structure	Smaller cages 5.5-8.8 Larger cages 25-29	3,100	[184]
MIL-101(Cr)	$CrCl_3·6H_2O$	H_2BDC	H_2O	Enhanced MTN zeolite topology structure	Smaller cages 5.5-8.8 Larger cages 29-34	3,549	[185]
Mg-MOF-74	$Mg(CH_3COO)_2$	H_4dhtp	DMF/ethanol/H_2O	HCB topology structure	7-13	> 1,000	[186]
MIL-125(Ti)	$Ti(OC_4H_9)_4$	H_2BDC	DMF/ CH_3OH	HCB topology structure	3.7-4.8	1,200-1,350	[187]
MOF-303 Al	$AlCl_3·6H_2O$	H_2PDC	NaOH aqueous solution	XHH topology structure	6	900-1,000	[188]

MOFs: Metal-organic frameworks; DMF: N, N-dimethylformamide; BDC: 1,4-benzene dicarboxylate; BPDC: biphenyl-4,4′-dicarboxylicacid; TCPP: tetrakis (4-carboxyphenyl)porphyrin; DEF: N, N-diethylformamide; ICA: iminazole-2-carboxaldehide; PVP: polyvinylpyrrolidone; SHP: square honeycomb paddlewheel; SPN: square planar network; GLS: generalized lattice structure; SOD: sodalite; RHO: rhombohedral; GME: gmelinite; TBO: tetrahedral bipyramid octahedron; MTN: multi-triangulated network; HCB: hexagonal close-packed; XHH: extended honeycomb hexagonal.

IL{1-ethyl-3-methylimidazolium bis[(tri-fluoromethyl)sulfonyl]imide [EMIM][TFSI]}/fluoroethylene carbonate (FEC) with poly(ethylene glycol) diacrylate, pentaerythritolte tetrakis (mercaptoacetate), and azobisisobutyronitrile (AIBN).

Vacuum filtration

Vacuum filtration is also applicable to grafting MOF particles onto different substrates. Liu *et al.*[192] prepared an asymmetric Cu-TCPP/MXene composite separator using vacuum filtration. Similarly, Huang *et al.*[143] used an electrospun separator to vacuum filtrate mixed UIO-66/carboxymethyl cellulose (CMC) aqueous dispersion, obtaining a UIO-66-based separator [Figure 7B]. Han *et al.*[193] also prepared MOFs@PVDF-based QSSEs using vacuum filtration method. Mg-MOF-74/polyethylene pyrrolidone dispersed in ethanol was filtered by a PVDF membrane; immersing the MOFs@PVDF membrane in the electrolyte solution can render MOFs@PVDF-based QSSEs.

In-situ gelation method

Lei *et al.*[144] prepared UIO-66-based QSSE by *in-situ* gelation. Firstly, $AlCl_3$ and acrylamide were mixed in methylene chloride (MC) for the complexation between acrylamide and $AlCl_3$, and then UIO-66 and AIBN (initiator) were added. Subsequently, the solution was poured onto aluminum foil and placed in a glove box for solidification and polymerization, obtaining MOF@GPE (gel polymer electrolyte). Similarly, Zhang *et al.*[145] introduced HKUST-1 to prepare QSSE [Figure 7C]. Benzophenone (BP) (photoinitiator), HKUST-1, and PEO were thoroughly mixed, and then polymerized under ultraviolet (UV) irradiation due to the insertion of free radicals generated by BP into PEO molecular chains. Finally, the gel is transferred to the glove box and soaked in the LE to obtain QSSE modified by HKUST-1. Liu *et al.*[165] also obtained UIO-67-based QSSEs by mixing PVDF-HFP/acetone and UIO-67/N,N-dimethylacetamide, followed by solvent evaporation and drying.

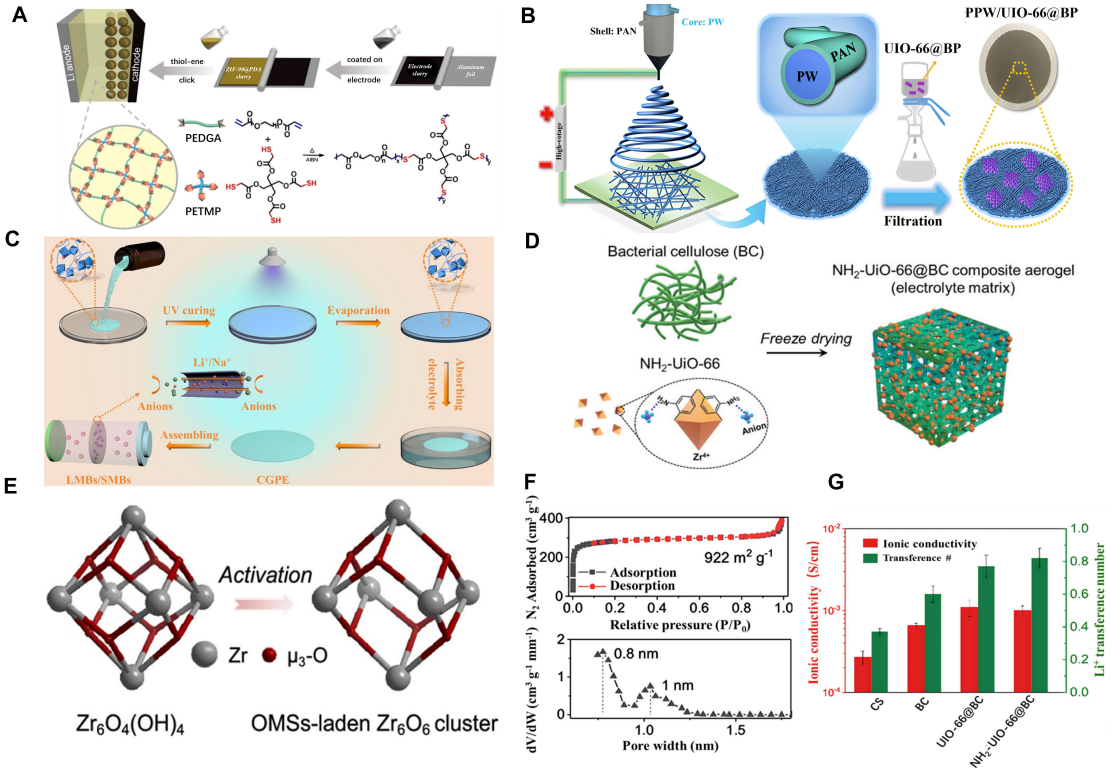

Figure 7. (A) Scrape coating MOF onto a commercial separator; (B) Vacuum filtration of MOFs on an electrospun separator; (C) *In situ* gelation of MOF with polymer precursor solution to obtain MOF-based gel polymer electrolyte; (D) Preparation of MOF-based aerogel electrolyte; (E) Increasing the number of OMSs in Zr-based MOFs via thermal activation; (F) N_2 isotherms (top) and corresponding pore size distribution (bottom) of chemically-activated UiO-66; (G) Increased ion conductivity and cation transference number of electrolytes containing chemically activated MOF. (A) is quoted with permission from Wang *et al.*[154]; (B) from Huang *et al.*[143]; (C) from Zhang *et al.*[145]; (D,F,G) from Fu *et al.*[153]; and (E) from Lu *et al.*[152]. MOF: Metal-organic frameworks.

Aside from hydrogels, MOF aerogels can also be adopted to prepare QSSEs. Due to the excellent liquid storage capacity and high tensile strength of aerogels, batteries using aerogel QSSE have excellent performance. Fu *et al.*[153] introduced NH_2-UIO-66 into bacterial cellulose (BC)-modified aerogel electrolytes to optimize the performance of high-pressure LMBs [Figure 7D]. Aqueous MOF dispersion was added into BC dispersed in deionized water. After freeze-drying, hot press and immersing in an electrolyte containing lithium ions, NH_2-UIO-66@BC composite aerogel electrolyte is obtained.

Incorporating MOFs into battery electrolytes can be realized by either grafting MOFs onto separators (e.g., coating and filtration) or dispersing them in gel electrolytes. However, uniform dispersion of MOFs on separators (or in QSSEs) should be guaranteed to fully harvest the merits of MOF-based separators for LMBs.

Activation of MOF-based separators

Aside from tunable structures, the numerous open metal sites (OMSs) of MOFs used in separators are also pivotal to improving electrochemical performance in batteries. OMSs of MOFs can anchor anions, catalyze and adsorb by-products, suppress shuttle effects, and improve ion mobility. Increasing the number of OMSs can significantly increase the electrochemical performance of MOF-based separators. Activating MOFs, therefore, should be considered to create more OMSs. The common methods (e.g., thermal activation and chemical activation) to activate MOFs for separators/QSSEs will be narrated in this section.

Thermal activation

Lu *et al.*[152] obtained UIO-66 with more Lewis acid sites and high activation area through thermal activation [Figure 7E]. UIO-66 can be thermally activated without collapsing the initial structure, and the thermal activation condition of UIO-66 was optimized to 300 °C for 24 h. The thermally activated UIO-66 has an increased number of active sites, enabling GPE with higher ion conductivity and cation transference numbers for QSSLMB. Férey *et al.*[194] utilized thermal activation to increase the specific surface area and volume of MIL-101 (Cr) micropores, resulting in excellent adsorption performance. Xu *et al.*[195] used a simple thermal activation method to clean the coordination water molecules inside the framework of synthesized Mn-MOF-1 with methanol, and then heated it at 120 °C to obtain an activated sample with more OMSs. MOFs with poor stability can be thermally activated in a protective atmosphere. Zhang *et al.*[196] conducted thermal activation under different protective atmospheres, and found that using CO resulted in the highest activity of CuBTC [1,3,5-benzenetricarboxylic acid (BTC)], forming more pores and effective Cu_2O during activation. This viewpoint can be considered for the thermal activation of other MOFs to optimize the activation effect. Thermal activation can expose and activate the OMSs in MOFs by removing pore filling guest molecules and pre-coordinated solvent molecules from open coordination sites.

Chemical activation

MOF-based separators can increase the transference number of cations and ionic conductivity, which can be realized via chemical activation of MOFs by grafting anionic organic ligands[197]. Fu *et al.*[153] replaced BDC with 2-aminoterepthalic acid when synthesizing UIO-66, producing NH_2-UIO-66 with smaller pores [Figure 7F], larger specific surface area, higher ion conductivity [Figure 7G], and more Lewis acid sites, effectively accelerating ion conduction and inhibiting dendrite growth, enabling improved performance in LMBs. Planchais *et al.*[198] introduced -COOH groups into UIO-66 to improve the hydrophilicity of UIO-66, resulting in better proton conductivity. Yang *et al.*[199] also modified commercial glass fibers (GF) with carboxyl functionalized UiO-66-$(COOH)_2$ (UC), rendering a novel ion selective separator (UC/GF) that suppresses polyiodides shuttle and improves ionic conductivity in zinc iodine batteries. Another common chemical activation method is to introduce sulfonic acid groups on MOFs. Ruan *et al.*[200] replaced H_2BDC with H_2BDC-SO_3Na during the synthesis of UIO-66, successfully preparing UiO-66-SO_3H with more Lewis acid sites and a higher number of micropores, offering more active sites. In addition to introducing active functional groups, metalizing MOFs is also viable for chemical activation. By adding a mixed solution of $FeCl_3$ and DMF to MOF-525 and MOF-545 and subsequent heating, Morris *et al.*[201] successfully prepared metalized MOF-525-Fe and MOF-545-Fe, with increased porosity and extremely high stability while retaining the properties of the original MOFs. Kim *et al.*[202] also exposed the active sites of HKUST-1 and Cu-MOF-2 by immersing in MC, which can replace impurities coordinating the active sites, thus exposing the active sites of HKUST-1 and Cu-MOF-2 after the self-decomposition of MC.

Chemical activation of MOFs can not only remove guest molecules from the active site, but also introduce defects on the organic ligand. Controlling the generation of ligand defects within UiO-66 can increase the ionic conductivity by nearly three orders of magnitude[163], emphasizing the importance of chemical activation of MOFs to design superior QSSE. In addition to thermal activation and chemical activation, other methods to activate MOFs include solvent exchange[203,204], freeze-drying[205,206], supercritical CO_2 exchange[206], *etc.*[207], offering new possibilities of MOF modification toward favorable MOF-based separators or QSSEs.

Challenges and strategies in industrial scale-up of MOFs

Although substantial research has been dedicated to MOFs[208-212], there are limited options for commercially available MOFs. Key considerations for scalable MOF production include the selection of metal ions and organic linkers, the use of industrial hydrothermal reactors, and adoption of green solvents and synthesis

methods. For large-scale MOF synthesis, choosing metal ions that are both accessible and cost-effective is critical, with metal oxides and sulfates generally preferred due to their stability, while chlorides and nitrates pose corrosion and safety risks, respectively. Simple organic linkers such as terephthalic acid are also advantageous for their availability and cost-efficiency[213]. The most commonly used hydrothermal or solvothermal synthesis is highly suitable for scaling and adaptable for industrial continuous stirred tank reactors, as demonstrated by McKinstry *et al.*, who achieved a production rate of approximately 1,000 kg m^{-3} per day of high-quality MOF-5 using a scalable system[214]. However, this approach often requires large amounts of solvent. Mechanochemistry presents a promising alternative, producing MOFs through mechanical mixing with minimal or no solvent, which is both environmentally friendly and energy efficient. Klimakow *et al.* produced copper-based MOFs (HKUST-1 and MOF-14) using a ball mill and minimal ethanol, while Tanaka *et al.* created ZIF-8 via solvent-free grinding, thus reducing potential impurities[215,216]. When solvents are required, green options such as water are preferred to organic solvents to reduce toxicity; for example, Chen *et al.* synthesized a zirconium-based MOF (UiO-66-NO_2) in water, and Cadot *et al.* achieved a high-quality nickel-based MOF with a 92% yield in an aqueous solution, yielding 680 kg m^{-3} per day[217,218]. Overall, careful selection of metal sources, synthesis techniques, and solvent types will be essential for scalable, cost-effective, and sustainable MOF production, enabling practical industrial applications.

THE APPLICATION OF MOF-BASED SEPARATORS IN QSSLMBS

Incorporating MOFs into separators addresses key challenges such as improving ionic conductivity[193,219], enhancing mechanical stability[220,221], and suppressing dendrite formation[222,223], thereby boosting the performance and safety of LMBs[220,224]. This section explores the use of pristine MOFs[220,225], MOF composites[226,227], and MOF derivatives[228,229] as separators in different types of QSSLMBs, highlighting their distinct advantages and recent advances.

Original MOF-based separators

Pristine MOFs, used as separators, offer high porosity and large surface area, facilitating efficient lithium-ion transport and dendrite inhibition. For example, Li *et al.*[230] prepared Cr-MOFs [MIL-88B(Cr) and MIL-101(Cr)] as coatings for PPSs [Figure 8A]. These Cr-MOF-coated separators showed superior thermal stability (160 °C), improved wettability (contact angle of 9.22°), and higher ionic conductivity (~3 mS cm^{-1}) compared to conventional inorganic Al_2O_3 coatings. Full-cell tests using LFP cathodes demonstrated that Cr-MOF-coated separators maintained high discharge capacity (70 mAh g^{-1}) at 10C. MIL-101(Cr) exhibited better performance than MIL-88B(Cr) due to its higher Brunauer-Emmett-Teller surface area (1,846 m^2 g^{-1} *vs.* 578 m^2 g^{-1}) and larger pore volume (0.884 cm^3 g^{-1} *vs.* 0.264 cm^3 g^{-1}). This enhanced porosity increased LE absorption, improving electrode wettability and reducing charge transfer resistance [90.39 Ω for MIL-101(Cr) *vs.* 126.14 Ω for MIL-88B(Cr)]. These findings highlight the importance of MOF porosity in designing high-performance and durable separators for LMBs.

Original MOFs have been demonstrated to significantly expand the electrochemical window, enabling their stable operation in high-voltage batteries such as Li//NCM (lithium nickel manganese cobalt oxides) batteries[231-234] . Chang *et al.*[231] reported a novel LE comprising desolvated Li^+ (referred to as "desolvated Li^+ electrolyte") by exploring interactions between Li^+ and $TFSI^-$ ions with dimethoxyethane (DME) solvent in the narrow (~2.9 Å) channels of ZIF-7 MOF. Unlike conventional LEs, this novel electrolyte consists of a "frozen-like" inactive solvent and crystalline lithium salt, primarily composed of desolvated Li^+ [Figure 8B]. As a result, the electrochemical stability of the desolvated Li^+ electrolyte is significantly enhanced, extending from 3.8 V to 4.5 V [Figure 8C]. High-voltage LMBs ($LiNi_{0.8}Co_{0.1}Mn_{0.1}O_2$//Li) using this electrolyte exhibit excellent retained capacity 170 mAh g^{-1} over 200 cycles [Figure 8D]. Remarkably, the cathode-electrolyte interphase layer is barely detectable on the NCM-811 cathode surface, likely due to the absence of free

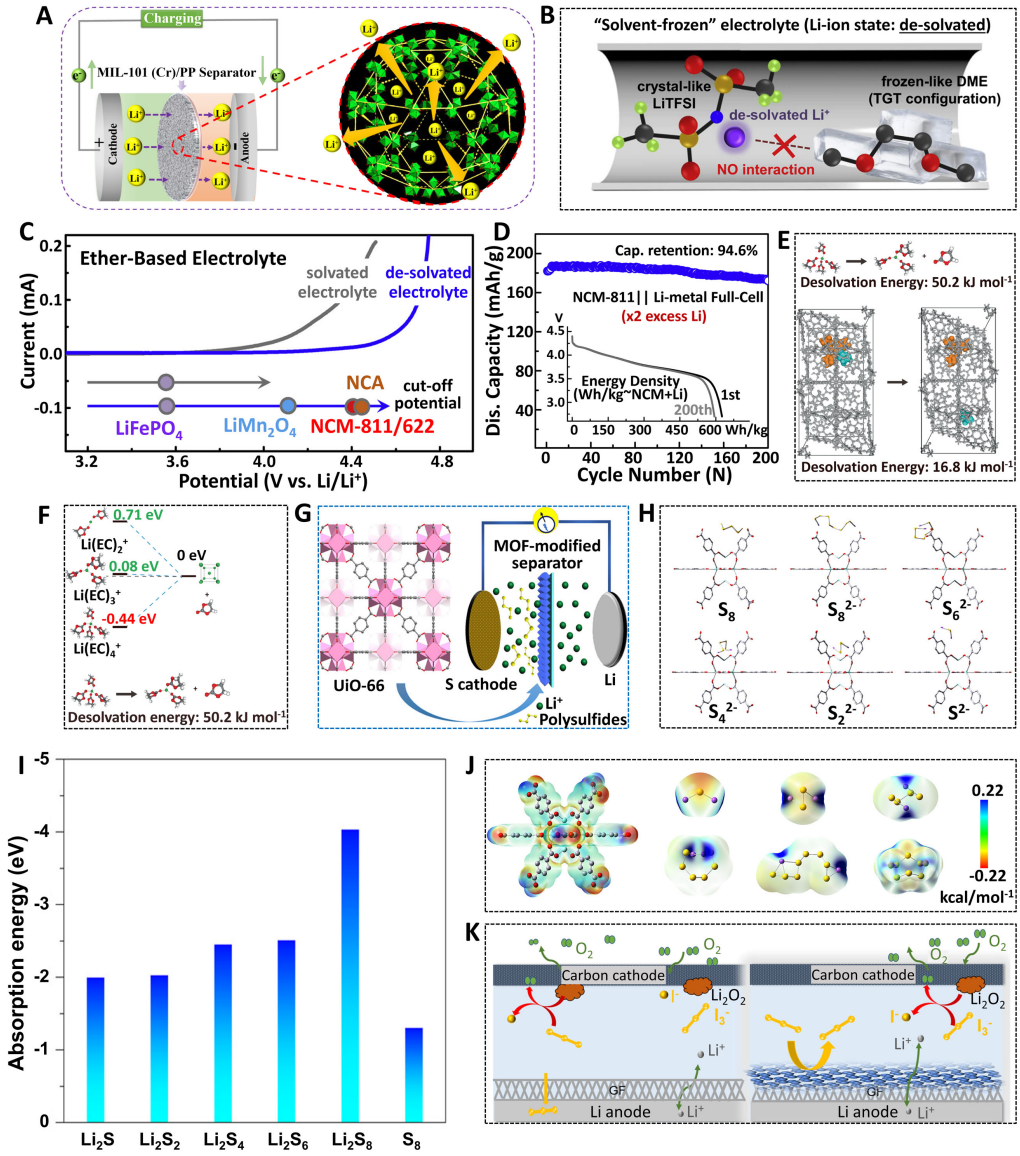

Figure 8. (A) Schematic representation of Li^+ transportation through MIL-101(Cr)/PP separator; (B) Schematic illustration for the configuration of the designed "Li^+ desolvated electrolyte"; (C) The linear sweep voltammetry (LSV) curves of typical "Li^+ solvated ether-based electrolytes" and "desolvated electrolyte"; (D) The discharge capacity against cycle number collected from Li//NCM-811 full-cells using "Li^+ desolvated electrolyte"; (E and F) Desolvation energy of $Li(EC)_4^+$ to $Li(EC)_3^+$ and EC molecule in bulk LE and UiO-66 pores, respectively; (G) The UiO-66-modified PP separator for Li-S batteries; (H) Geometries of atomic model configurations and (I) corresponding adsorption energy between polysulfides and UiO-66; (J) Molecular surface electrostatic potential (ESP) of UiO-66 and polysulfides; (K) The HKUST-1-modified GF separator for Li-O_2 batteries. (A) is quoted with permission from Li *et al.*[230]; (B-D) from Chang *et al.*[231]; (E and F) from Sheng *et al.*[232]; (G-J) from Fan *et al.*[235]; (H) from Fan *et al.*[238]. EC: Ethylene carbonate; GF: glass fibers.

solvent in the desolvated Li^+ structure.

To gain deeper insight into the desolvation mechanism and its role in stabilizing Li^0, Sheng *et al.*[232] employed density functional theory (DFT) calculations to model the dissociation and reduction of solvated Li^+ within UiO-66 MOF channels and bulk LE [$LiPF_6$ in ethylene carbonate (EC)]. The energy required to dissociate $Li(EC)_4^+$ to $Li(EC)_3^+$ and one EC molecule on UiO-66 is approximately 16.8 kJ mol^{-1}, significantly lower than the corresponding energy in bulk electrolyte (50.2 kJ mol^{-1}) [Figure 8E]. This suggests that

UiO-66 weakens or partially dissociates solvent-Li^+ complexes. Additionally, the calculated reduction potentials for the partially desolvated $Li(EC)_3^+$ and $Li(EC)_2^+$ species were 0.08 V and 0.71 V, respectively, while the reduction potential of $Li(EC)_4^+$ in bulk LE was -0.44 V [Figure 8F]. This indicates that after partial EC dissociation in MOF channel, the reduction of Li^+ from $Li(EC)^{3+}$ to Li^0 becomes energetically competitive with the reduction of solvent molecule.

Original MOFs are also widely used as effective separators in Li-S batteries[235-237]. Fan *et al.* synthesized uniform UiO-66 (Zr) MOF particles via solvothermal reaction for Li-S batteries[235] [Figure 8G]. UiO-66 effectively mitigates the shuttle effect due to its strong physical and chemical interactions with dissolved polysulfides. Li-S cells with UiO-66-coated PPSs maintained a specific capacity of 586 mAh g^{-1} after 500 cycles at 0.5 C, with a Coulombic efficiency near 100%. DFT simulations reveal that Li_2Sn ($4 < n < 8$) species penetrate UiO-66's ~9.1 Å pores and interact with the pore walls, reducing pore size and preventing further polysulfide infiltration [Figure 8H]. Adsorption energy calculations indicate strong chemisorption, with values below -2 eV for all polysulfides except S_8 [Figure 8I]. This is attributed to strong interactions between Li^+ ions and oxygen atoms in UiO-66, as well as between S atoms and MOF hydrogen atoms. Electrostatic potential (ESP) mapping confirms these interactions, showing Coulombic attraction between Li^+ and UiO-66 oxygen atoms [Figure 8J]. These findings demonstrate that the combined effects of chemisorption and physical confinement in UiO-66-coated separators effectively suppress the shuttle effect, enhancing the stability and cycling performance of Li-S batteries. This highlights the importance of MOF for Li-S applications.

MOFs with small pore sizes have also emerged as effective filtration materials for suppressing anion shuttling in lithium-oxygen (Li-O_2) batteries. For example, Fan *et al.*[238] fabricated a HKUST-1 MOF-coated GF separator to inhibit redox-active ion transport associated with I^-/I_3^- species in Li-O_2 cells [Figure 8K]. The three-dimensional stacking and interwoven structure of HKUST-1 serve as a physical barrier against anion migration. Additionally, HKUST-1 exhibits multiple Lewis acid sites, while I^-/I_3^- species are characterized as Lewis bases. This combination of physical barrier modification and Lewis acid-base interactions effectively impedes the transport of I^-/I_3^- ions while preserving Li^+ conductivity and ensuring the chemical stability of the separator. The HKUST-1/GF separator demonstrates high ionic conductivity (1.35×10^{-3} S cm^{-1}) and a Li^+ transference number of 0.46. Li-O_2 cells utilizing the HKUST-1/GF separator achieve a six times longer cycle life, sustaining 180 cycles in an I^-/I_3^--based electrolyte.

The varying pore sizes and compositions of original MOFs significantly affect the ionic conductivity of QSSEs in LMBs. During the synthesis of Mg-based MOFs, Aubrey *et al.*[239] modified the linkers, producing Mg_2(dobdc) and Mg_2(dobpdc) with pore sizes of 13 Å and 21 Å, respectively [Figure 9]. Mg_2(dobpdc) shows an ionic conductivity of ~10^{-4} S cm^{-1}, more than double that of Mg_2(dobdc), due to its larger pores and higher surface area, which enhance Li salt absorption and inhibit side reactions. This highlights the critical role of pore size and composition in improving ionic conductivity in MOF-based QSSEs. Additionally, ionic conductivity is influenced by the MOF framework's structural properties and interfacial effects from trace solvents retained in the pores[240,241].

MOF composites-based separators

MOF composites combining MOFs with other materials such as polymers or inorganic particles leverage synergistic effects to optimize ionic conductivity, mechanical strength, and thermal stability, providing enhanced performance for QSSLMBs. For example, incorporating MOFs into polymer matrices has significantly improved separator performance[242-246]. Lu *et al.*[242] developed a hybrid separator by integrating a bifunctional MOF material (MOF-2) into a PEO matrix. MOF-2, prepared from two different

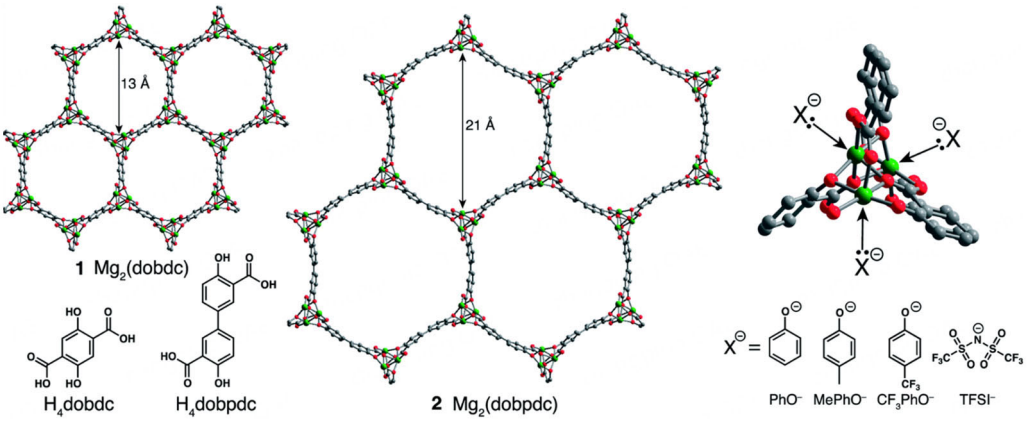

Figure 9. Pore structure and surface modification of Mg_2(dobdc) and Mg_2(dobpdc) as QSSEs. This figure is quoted with permission from Aubrey *et al.*[239]. QSSEs: Quasi-solid-state electrolytes.

functionalized UiO-66 materials containing carboxyl and amine groups, respectively, in combination with PEO [Figure 10A] showed higher ionic conductivity (5.20×10^{-4} S/cm) than pristine PEO (1.11×10^{-4} S/cm). This improvement is likely due to the presence of MOFs, which disrupt the arrangement of PEO chains, reducing the crystallinity of the electrolyte. Additionally, MOFs can serve as supplementary ion channels, enhancing lithium-ion transport. Interestingly, the ionic conductivity of QSSE with MOF-2 surpassed that of QSSE containing individual MOFs such as UiO-66-COOH or UiO-66-NH_2. In MOF-2, amide bonds formed between acid and amino groups create long MOF chains within the QSSE, facilitating rapid ion transport through a network where the polymer serves as the primary conduction channel. As such, $LiFePO_4$||Li full cells assembled with this composite separator showed 98.45% capacity retention at 149.92 mA h/g after 100 cycles at 1 C, significantly higher than those made with pristine PEO and single UiO-66 MOF [Figure 10B]. Furthermore, the electrochemical window increased by about 40% (from 3.5 V to 5.0 V), and the lithium-ion transference number increased by 80% (from 0.20 to 0.36 at 60 °C) after replacing pristine PEO with MOF-2@PEO. Another study by Guo *et al.*[243] reported a HKUST-1 [$Cu_3(BTC)_2$]-coated Celgard separator (PSS@HKUST-1/Celgard) [polystyrene sulfonate (PSS)] for high-performance Li-S batteries. HKUST-1, with its large pore structure (~8 nm), is known for its high polysulfide absorption capability, while PSS with giant sulfonate groups, combined with HKUST-1, enables fast and efficient Li-ion transport, rendering PSS@HKUST-1 membrane with ion conductivity 71% higher than the conventional Celgard separator. A Li-S battery with this composite separator showed a highly reversible capacity with an average fading rate of 0.05% over 500 cycles at 0.5 C, and a high areal capacity over 7 mA h cm^{-2}.

Besides polymer-MOF composites, inorganic-MOF composites have also been explored for their superior mechanical and thermal properties[247,248]. Suriyakumar *et al.*[248] coated a mixture of UiO-66-NH_2 and SiO_2 particles on a commercial Celgard 2320 membrane, enhancing thermal stability, wettability, ionic conductivity, and electrochemical window, producing higher discharge capacity in Li-S cells. This is attributed to the electrostatic and/or hydrogen-bonding interactions between the polysulfides and UiO-66-NH_2@SiO_2. Additionally, the good permeability properties of the separator limit the self-discharge of Li-S cells, retaining up to 98.5% of the initial capacity after 40 h. Zhou *et al.* further applied separate coatings of Co-MOF and LLZO powder on different sides of polyimide (PI) separators for Li-S batteries[247] [Figure 10C]. Co-MOF adsorbs dissolved polysulfides due to its porous nature, while LLZO effectively prevents lithium dendrite growth. The Co_3O_4/PI/LLZO composite demonstrated good mechanical strength, flame retardancy, and excellent ionic conductivity, rendering Li-S cells with stable operation at 80 °C and

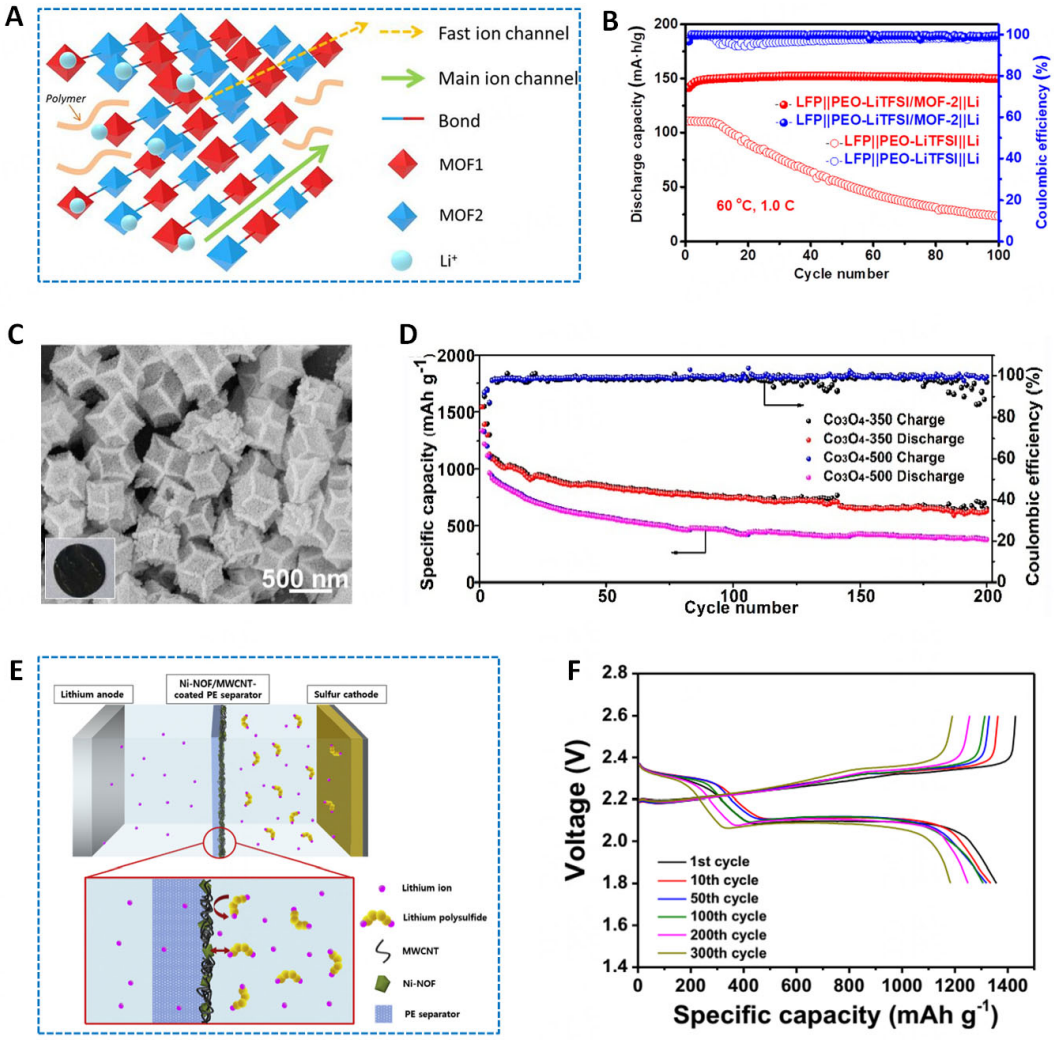

Figure 10. (A) Bifunctional MOF doped PEO composite electrolyte (PEO-MOF-2) for fast ionic transport; (B) Cycling stability of full cells with PEO-MOF-2 at 1 C; (C) SEM images of the Co_3O_4-350 polyhedron and Co_3O_4-350/PI/LLZO separator; (D) The cycling performances of Li-S cells using varied separator at room temperature; (E) Schematic illustration of Ni-MOF/MWCNT-coated PE separator for blocking lithium polysulfide migration to the lithium anode in the Li-S cell; (F) Charge and discharge curves of the Li-S cell with Ni-MOF/MWCNT-coated separator at 0.2 C rate. (A and B) are quoted with permission from Lu *et al.*[242]; (C and D) from Zhou *et al.*[247]; and (E and F) from Lee *et al.*[253]. MOF: Metal-organic framework; PEO: polyethylene oxide; MWCNTs: multi-walled carbon nanotubes; SEM: scanning electron microscope; PE: polyethylene.

great cycling stability of 800 mAh g^{-1} after 200 cycles [Figure 10D].

Additionally, MOFs combined with carbon-based materials have shown promising results in enhancing both mechanical properties and lithium-ion transport for LMBs[227,249-254]. Bai *et al.*[227] created a separator based on Cu-MOF@Graphene oxide (HKUST-1@GO), acting as an effective ion sieve in Li-S batteries that selectively screened Li^+ ions while preventing polysulfide shuttling. The three-dimensional channel structure of HKUST-1@GO contains highly ordered micropores with size (approximately 9 Å) significantly larger than lithium polysulfides (Li_2Sn, $4 < n \leq 8$) (2.09-2.39 Å), making the separator highly suitable for adsorbing and blocking polysulfides. The Li-S battery with this MOF-based separator exhibits a low-capacity decay rate (0.019% per cycle over 1,500 cycles), with virtually no capacity loss after the first 100 cycles. Lee *et al.*[253] also used multi-walled carbon nanotubes (MWCNTs) combined with Ni-based MOF to create separator

membranes for Li-S batteries [Figure 10E]. Ni-MOF particles effectively block lithium polysulfide shuttling due to strong interactions, while MWCNTs allow the reuse of reactive intermediates due to their high conductivity. Specifically, the Lewis acidic Ni^{2+} sites in Ni-MOF foster strong interactions with polysulfide anions, whose lone electron pairs impart soft Lewis basicity. As a result, Ni-MOF effectively traps lithium polysulfides through Lewis acid-base interactions. Additionally, MWCNTs not only compensate for the low electronic conductivity of Ni-MOF and enhance the electronic conductivity of trapped lithium polysulfides for subsequent electrochemical reactions, but also act as a physical barrier against lithium polysulfide migration. These synergistic effects result in a high discharge capacity of 1,358 mAh g^{-1} at the initial cycle for Li-S batteries [Figure 10F].

Similar to original MOFs, MOF composite-based separators also demonstrate excellent electrochemical stability under high-voltage operation. Chang *et al.*[10] developed a separator based on CuBTC MOF and poly(sodium 4-styrenesulfonate). Using advanced space-resolution spectroscopies, the prepared electrolyte exhibited significant aggregation beyond the standard saturation state (exceeding the lithium salt solubility limit) and primarily contained solvent-depleted contact ion pairs [Figure 11A]. This unique electrolyte structure significantly reduces solvent decomposition, resulting in exceptional electrochemical stability exceeding 5.4 V versus Li/Li^+ [Figure 11B]. Consequently, electrolyte decomposition on cathode was significantly suppressed while a thin and stable SEI layer was simultaneously formed on lithium metal anode during cycling, rendering high-voltage Li//NCM811 with long-term cycling performance, maintaining 170 mAh g^{-1} after 400 cycles [Figure 11C].

MOF composite-based separators have also been successfully applied in Li-O_2 batteries, delivering remarkable performance enhancements. For instance, Wang *et al.*[255] synthesized a MOF gel by combining UiO-66 with Li-COOH and coated it onto a PPS for $Ru(acac)_3$@Li-O_2 batteries. Through size and kinetic simulations, the pore size distribution of the gel MOF [UiO-66-$(COOLi)_2$] was primarily below 6.5 Å and between 11.0-13 Å, which is mostly smaller than the 12.6 Å length of $Ru(acac)_3$ [Figure 11D]. This size exclusion effect effectively inhibits the $Ru(acac)_3$ transport. When $Ru(acac)_3$ moves through the smaller channels, the polar -COO^- groups within the MOF tend to adsorb polar dimethyl sulfoxide (DMSO) molecules while repelling nonpolar $Ru(acac)_3$ molecules[255] [Figure 11E and F]. Simultaneously, the negatively charged -COO^- groups in the MOF channels facilitate the uniform transport of lithium ions, thereby improving the battery's overall performance. Notably, the $Ru(acac)_3$@Li-O_2 battery equipped with the MOF gel separator exhibited an ultralong cycle life of 410 cycles at a current density of 0.5 A g^{-1}, significantly superior to batteries using conventional Celgard separators.

MOF derivatives-based separators

MOF derivatives, which include chemically modified or transformed MOFs into other functional materials, represent an advanced approach in separator design. These derivatives often exhibit increased ionic conductivity, improved thermal stability, light weight, and high porosity addressing specific challenges in LMBs, especially Li-S batteries. Converting MOFs into porous carbon or metal oxide materials is a common strategy.

For example, Guang *et al.*[256] prepared double-shelled hollow N-doped porous carbon polyhedrons (DSxHNC) derived from ZIF-8@ZIF-67 core-shell nanocrystals by high-temperature treatment (465-750 °C) [Figure 12A]. A thin, dual-functional interlayer was doctor-bladed onto a commercial PPS with negative-pressure infiltration. The prepared DSxHNC exhibits a unique hollow structure, making it lightweight and suitable for large-scale production and packaging. The abundant N-doped sites and widespread micro/mesopores of DSxHNC efficiently suppress Li polysulfide migration through synergistic

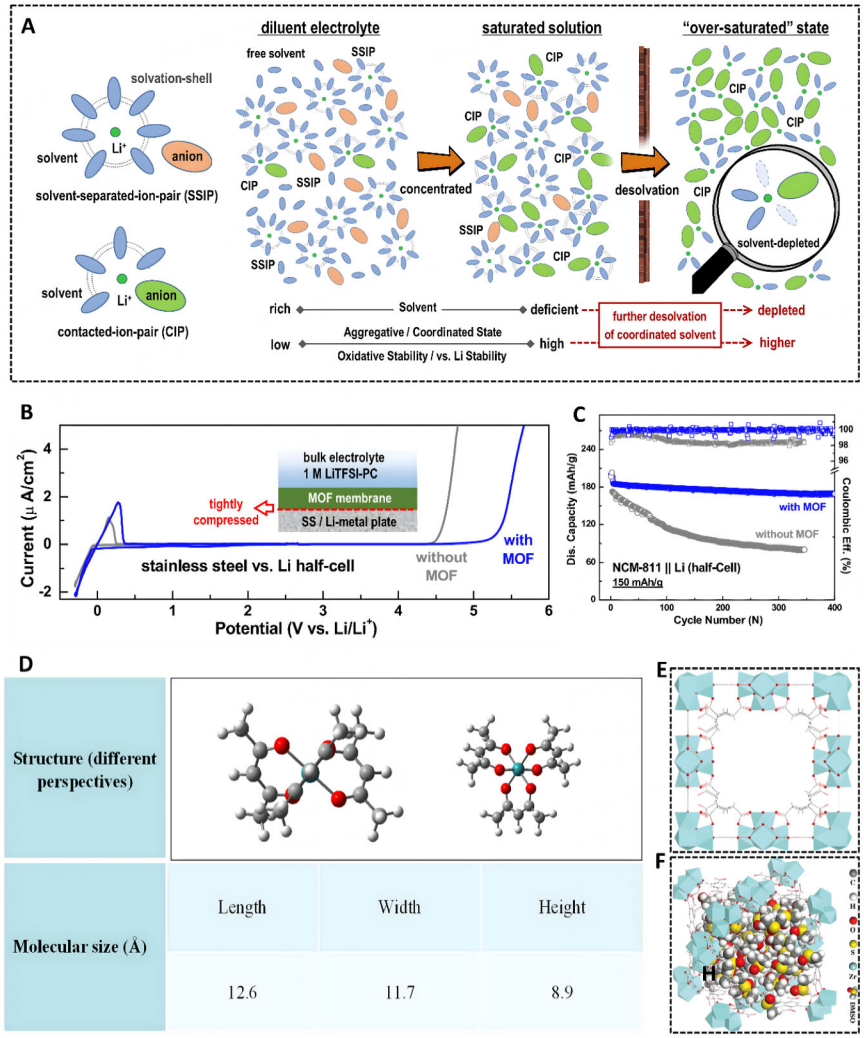

Figure 11. (A) The proposed design idea of further depleting solvent molecules within Li^+ solvation sheath; (B) LSV curves of typical electrolyte and the prepared solvent-depleted electrolyte in CuBTC MOF-PSS; (C) Cycling performance of the Li//NCM-811 half-cell using the MOF-based electrolyte; (D) Molecular structures at different angles and the sizes of $Ru(acac)_3$; (E and F) Schematic structures of UiO-66-$(COOLi)_2$ and DMSO located in UiO-66-$(COOLi)_2$. (A-C) is quoted with permission from Chang *et al.*[10]; (D-F) from Wang *et al.*[255]. MOF: Metal-organic framework; LSV: linear sweep voltammetry; DMSO: dimethyl sulfoxide; PSS: polystyrene sulfonate.

physical and chemical adsorption at both low (1.0 mg cm^{-2}) and high (3.1 mg cm^{-2}) sulfur loadings. Interestingly, the movement of Li polysulfide and the shuttling of Li^+ ions are regulated by adjusting the thickness and density of the dual shells, achieved through varying H_2 treatment times. When applied to Li-S batteries, the cells exhibited significantly improved high-capacity retention of 80% after 100 cycles at 0.2 C [Figure 12B and C].

Li *et al.* enhanced the separation efficiency of Celgard 2325 membranes by $NiCo_2S_4$@C[257] [Figure 12D], which was formed through heat treatment of Ni-Co-PTA in Ar gas and subsequent solvothermal reaction with Na_2S. The highly porous $NiCo_2S_4$@C nanocomposite not only possesses exceptional physical adsorption capabilities but also exhibits excellent polar chemical adsorption for Li polysulfides through interactions between the Ni and Co cations and S anions. Moreover, the $NiCo_2S_4$@C composite features three-dimensional electrical conductivity, abundant porosity, and a high specific surface area, significantly

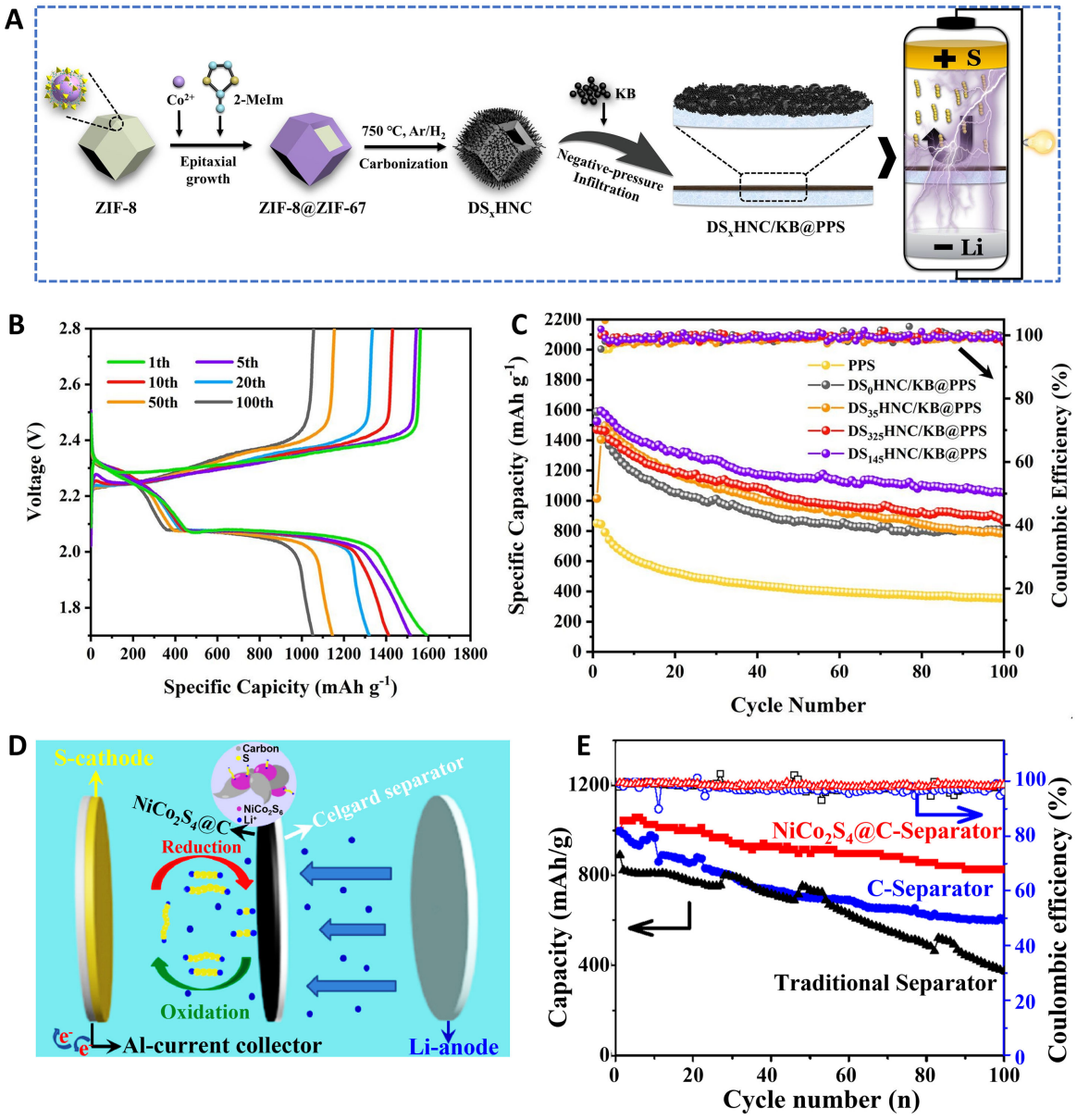

Figure 12. (A) Schematic illustration of the synthesis process of DSxHNC and DSxHNC/KB@PPS [ketjen black (KB)] and schematic representation of L-S battery employing the DSxHNC/KB@PPS; (B) Galvanostatic charge/discharge voltage profiles of DS_{145}HNC/KB@PPS at 0.2 C; (C) Cycling performances and Coulombic efficiencies of DSxHNC/KB@PPS and PPS at 0.2 C; (D) Schematic configuration of Li-S battery with $NiCo_2S_4$@C-modified separator; (E) Cyclic performance of the batteries assembled with $NiCo_2S_4$@C and other separators at 0.5 C. (A-C) are quoted with permission from Guang *et al.*[256]; and (D and E) from Li *et al.*[257]. DSxHNC: Double-shelled hollow N-doped porous carbon polyhedrons; PPS: polypropylene separator.

improving ionic/electronic conductivity and Coulombic efficiency. As such, $NiCo_2S_4$@C separators ensured Li-S batteries with a high initial capacity of 880 mAh g^{-1} at 0.5 C [Figure 12E] and excellent cycling stability, maintaining a capacity of up to 700 mAh g^{-1} after 200 cycles.

Additionally, other MOF derivatives have been synthesized and applied as effective separators in QSSLMBs. These include Co-based MOF-derived vertical Co_9S_8 hollow nanowall arrays grown on a Celgard separator[229], oxygenated MOF-derived nitrogen-doped microporous carbon (OMNC)[258], and Ni-MOF-

derived bamboo-like conductive carbon nitride[259]. All these materials share high porosity, excellent electrical conductivity, and superior ion transport properties, making them highly advantageous for use as separators in QSSLMBs. Despite these promising characteristics, research and application of MOF derivative-based separators in other lithium battery systems, such as Li-O_2 and high-voltage Li//NCM cells, remain limited. A comprehensive and systematic analysis of the challenges and advantages associated with using MOF derivatives in these advanced battery systems is essential to accelerate their practical implementation in the near future.

CONCLUSIONS AND OUTLOOKS

This review provides a comprehensive overview of the development of MOF-based QSSEs in recent years. In addition to the fundamental aspects of MOF-based QSSEs (application concepts, compositions, Li-ion transport mechanisms, and typical fabrication methods), the recent progress of three main types of MOF-based QSSEs, including Original MOF-based Separators, MOF Composite-based Separators, and MOF Derivative-based Separators, has been systematically classified and introduced. The role of MOFs in terms of ionic conductivity, stability, and performance in various structures is highlighted. Each type has its own advantages, disadvantages, and challenges, as shown in Tables 2-5. Some conclusions based on the information compiled and discussed in this review are as follows.

Performance advantages and contributions

MOF-based separators offer distinct advantages that overcome key challenges in QSSLMBs. These separators serve as robust physical barriers that effectively suppress dendrite formation on lithium metal anodes, mitigating risks of short circuits and enhancing battery durability. Their high surface area and tunable pore structures facilitate efficient ion transport, resulting in improved ionic conductivity and enhanced electrochemical performance. Original MOF-based separators have high ionic conductivity and good thermal stability due to the excellent physical and chemical adsorption properties of MOFs, which can trap trace LE within the nano-sized pores. MOF composite-based separators show excellent Li dendrite suppression and good interface compatibility with electrode surfaces. Additionally, MOF-derived materials provide versatility in composition and functionality, allowing for tailored designs that optimize the ionic conductivity and interface compatibility between separators and electrode materials, thereby maximizing battery efficiency.

Challenges and future directions

Despite the significant progress, several challenges remain to be addressed. The nature of trace solvents, which do not enter MOF pore structures and are highly flammable, presents challenges. Developing methods to balance these trace solvents in the system without affecting battery performance is an important future direction. Additionally, lithium dendrite formation and growth may occur during prolonged battery cycling, particularly at high current densities. The accumulation of lithium dendrites and the expansion of cracks can happen at MOF grain boundaries, surface defects, and connecting pores. MOF composite-based QSSEs exhibit high flexibility and good interface compatibility, but their thermal stability and low ionic conductivity limit their application in high-energy-density batteries. Although MOF derivative-based QSSEs have good electrochemical properties, the complex fabrication methods, low mechanical stability, decreased pore size, and undesirable interactions between LEs and by-products from MOF derivative synthesis make it challenging to design and apply them to specific LMBs. Furthermore, challenges remain in the production of MOFs for QSSEs. The cost of metal salts and linkers is a notable issue. The use of environmentally unfriendly solvents or cumbersome fabrication processes hinders large-scale production of MOFs and MOF-based QSSEs.

Table 2. Comparison of advantages and disadvantages of different types of MOF-based QSSEs

Type of MOF-based QSSEs	Advantages	Disadvantages
Original MOF-based separators	• Various structures and chemical compositions • High porosity • Wide electrochemical window • High mechanical strength • High thermal stability	• Low flexibility • Complex manufacturing process
MOF composites-based separators	• Good interface compatibility • Good solubility of lithium salts • High flexibility	• Low ionic conductivity • Relatively low mechanical strength • Relatively low oxidation potential
MOF derivatives-based separators	• High ionic and electrical conductivity • Wide voltage window • High lithium-ion transference number	• Complex manufacturing process • Relatively low mechanical strength • Relatively low porosity

MOFs: Metal-organic frameworks; QSSEs: quasi-solid-state electrolytes.

Table 3. Summary of original MOF-based separators

MOFs	Lithium salts	Type of batteries	σ (mS cm^{-1})	Electrochemical window (V)	Initial capacity (a mAh g^{-1} _ b C rate)	Capacity retention (a%_b cycles)	References
MIL-101(Cr)	$LiPF_6$	Li//LFP	-	-	71_5	99_200	[230]
UiO-66	LiTFSI	Li-S	-	-	587_0.5	99.85_500	[235]
UiO-66	LiTFSI	Li-S	-	-	1239_0.2	84_200	[236]
UiO-66-NH_2	$LiClO_4$	Li//LFP	0.207	4.52	136_1	97_500	[237]
UiO-66	LiO*t*Bu	-	0.018	-	-	-	[240]
MIL-121	$LiClO_4$		0.091	-	-	-	[241]
MOF-688	LiTFSI	-	0.34	-	-	-	[102]
UiO-66	$LiPF_6$	Li//LFP	0.06	5.2	127_0.2	88.2_100	[161]
MIL-100(Fe)	$LiClO_4$	-	0.9	-	-	-	[177]
UiO-67	$LiClO_4$	-	0.65	-	-	-	[177]
UiO-66	$LiClO_4$	-	0.18	-	-	-	[177]
MOF-5	$LiClO_4$	-	0.13	-	-	-	[177]
HKUST-1	$LiClO_4$	-	0.38	-	-	-	[177]

MOFs: Metal-organic frameworks; LFP: $LiFePO_4$.

Future outlook and research opportunities

With outstanding advantages in safety and high energy density, MOF-based QSSEs show great promise for LMBs. Additionally, due to their flexibility and portability, these QSSEs can be applied in specific fields such as mobile electronic devices, drones, and more. Currently, MOF-based QSSLMBs are still in the early stages of research and development, and this new technology is not yet suitable for mass production. The following are deeper discussions on future directions for the development and commercialization of these batteries:

• Exploration of novel MOF structures and compositions: Exploring novel MOF structures and compositions is critical for improving the performance and cycling stability of batteries. Future research should focus on developing MOFs with tailored pore sizes, surface functionalities, and ion-conducting frameworks to address specific challenges and improve the performance of various LMBs, such as high-voltage Li-NCM, Li-S, and Li-O_2 systems. Advanced computational simulations and machine-learning models can accelerate the identification and design of next-generation MOFs with superior ionic

Table 4. Summary of MOF composite-based separators

MOFs	Other materials	Type of batteries	σ (mS cm^{-1})	Electrochemical window (V)	Initial capacity a (mAh g^{-1} _ b C rate)	Capacity retention (a%_b cycles)	References
HKUST-1	GO	Li-S	-	-	1126_0.5	72_100	[227]
UiO-66-NH_2 @UiO-66-COOH	PEO	Li//LFP	0.52	5	152.3_1	98.45_100	[242]
HKUST-1	polystyrene sulfonate (PSS)	Li-S	0.0105	-	1278_0.5	60.6_500	[243]
UiO-66	Nafion	Li-S	-	-	1127.4_0.1	75.5_200	[244]
Cu-BTC	NSP	Li-S	-	-	1279_1	78.2_1000	[245]
UiO-66	SO_3Li	Li-S	-	-	1020_0.5	56.8_500	[246]
Co-MOF	PI/LLZO	Li-S	-	-	1132_0.1	55.6_200	[247]
UiO-66-NH_2	SiO_2	Li-S	-	-	1400_0.1	42.9_100	[248]
Zn-MOF	GO	Li-S	-	-	1118_1	70_200	[249]
$Co(acac)_2$	PAN	Li-S	-	-	1102_0.2	91.5_50	[250]
Ni-MOF	MWCNT	Li-S	-	-	1183_0.2	87.1_300	[253]
N-Ti_3C_2	MXene	Li-S	-	-	1018_0.5	70.3_500	[254]

MOFs: Metal-organic frameworks; LFP: $LiFePO_4$; PEO: polyethylene oxide; LLZO: $Li_7La_3Zr_2O_{12}$; PI: polyimide; MWCNTs: multi-walled carbon nanotubes; GO: graphene oxide; NSP: negative charged sulfonic polymer; PAN: polyacrylonitrile.

Table 5. Summary of MOF derivative-based separators

MOFs	MOF derivatives	Type of batteries	σ (mS cm^{-1})	Electrochemical window (V)	Initial capacity (a mAh g^{-1} _ b C rate)	Capacity retention (a%_b cycles)	References
Co-MOF	Co_9S_8 nanowall	Li-S	-	-	1385_0.1	85.9_200	[229]
ZIF-8@ZIF-67	DS_xHNC	Li-S	-	-	1592.9_0.2	66_100	[256]
Ni-Co-PTA MOF	$NiCo_2S_4$@C	Li-S	-	-	1000_0.5	83_100	[257]
ZIF-8	OMNC	Li-S	-	-	1257.1_0.5	59_300	[258]

MOFs: Metal-organic frameworks; DSxHNC: double-shelled hollow N-doped porous carbon polyhedrons; OMNC: oxygenated MOF-derived nitrogen-doped microporous carbon.

conductivity and chemical stability. Furthermore, to leverage the advantages of different MOFs, integrated structures, such as binary MOFs, MOF composites, MOF derivatives, or combinations of two or three of these, should be fabricated and analyzed to further enhance the performance and lifespan of LMBs.

• Development of innovative synthesis techniques: Conventional MOF synthesis often involves complex procedures and hazardous solvents. Future efforts should prioritize the development of cost-effective, scalable, and environmentally sustainable synthesis methods. Green synthesis approaches, such as solvent-free or aqueous-phase methods, may provide viable solutions for large-scale MOF production while maintaining high performance.

• In-depth study of Li-ion transport mechanisms: The Li-ion transport mechanism in MOF-based QSSEs directly affects battery performance and lifespan. Different types of MOFs have distinct Li-ion transport pathways. While some reports have identified main ion transport pathways in MOF-based QSSEs, the ion transport mechanisms will be more complex when MOFs are composited. This requires advanced methods for analysis and evaluation, such as MD simulations, solid-state NMR, *in-situ* X-ray photoelectron

spectroscopy, *in-situ* Raman spectroscopy, and more.

• Enhancing the ionic conductivity of MOF-based QSSEs: Despite studies focusing on improving Li^+ conductivity, the room-temperature conductivity in most MOF-based QSSEs remains relatively low (10^{-5} S cm^{-1} to 10^{-4} S cm^{-1}) compared to LEs (> 10^{-3} S cm^{-1}). New designs have the potential to improve the ionic conductivity of MOF-based QSSEs, such as incorporating one-dimensional nanostructures with MOFs, mixing MOFs with different pore sizes, or combining various types of MOFs. These approaches offer promising potential for future development.

• Enhancing cost-effectiveness and scalability: Emphasizing affordable raw materials and cost-effective synthesis techniques will enhance the commercial viability of MOF-based QSSRs. Exploring the potential and compatibility of MOFs in various battery systems can expand their applications. Collaborative efforts between academia and industry could facilitate the transition from laboratory-scale research to commercial implementation.

DECLARATIONS

Authors' contributions

Conceived and wrote the manuscript: Nguyen, M. H.; Niu, C.; Ngo, N. M.
Reviewed the manuscript and acquired funding: Chen, J.; Park, S.

Availability of data and materials

Not applicable.

Financial support and sponsorship

This work was supported by the National Research Foundation of the Republic of Korea (Project. No. RS-2023-00217581), Samsung Research Funding & Incubation Center of Samsung Electronics (Project No. SRFC-MA2202-04), the National Natural Science Foundation of China (No. 52202320), the Shandong Excellent Young Scientists Fund Program (Overseas) (2023HWYQ-060), and the Fundamental Research Funds for the Central Universities (No. 202201013153).

Conflicts of interest

All authors declared that there are no conflicts of interest.

Ethical approval and consent to participate

Not applicable.

Consent for publication

Not applicable.

REFERENCES

1. Armand, M.; Tarascon, J. Building better batteries. *Nature* **2008**, *451*, 652-7. DOI PubMed
2. Goodenough, J. B.; Park, K. S. The Li-ion rechargeable battery: a perspective. *J. Am. Chem. Soc.* **2013**, *135*, 1167-76. DOI PubMed
3. Tarascon, J. M.; Armand, M. Issues and challenges facing rechargeable lithium batteries. *Nature* **2001**, *414*, 359-67. DOI PubMed
4. Aravindan, V.; Gnanaraj, J.; Madhavi, S.; Liu, H. K. Lithium-ion conducting electrolyte salts for lithium batteries. *Chem. Eur. J.* **2011**, *17*, 14326-46. DOI PubMed
5. Li, M.; Wang, C.; Chen, Z.; Xu, K.; Lu, J. New concepts in electrolytes. *Chem. Rev.* **2020**, *120*, 6783-819. DOI

6. Qian, J.; Henderson, W. A.; Xu, W.; et al. High rate and stable cycling of lithium metal anode. *Nat. Commun.* **2015**, *6*, 6362. DOI PubMed PMC
7. Chang, Z.; Qiao, Y.; Deng, H.; Yang, H.; He, P.; Zhou, H. A stable high-voltage lithium-ion battery realized by an in-built water scavenger. *Energy. Environ. Sci.* **2020**, *13*, 1197-204. DOI
8. Jiao, S.; Ren, X.; Cao, R.; et al. Stable cycling of high-voltage lithium metal batteries in ether electrolytes. *Nat. Energy.* **2018**, *3*, 739-46. DOI
9. Zheng, J.; Engelhard, M. H.; Mei, D.; et al. Electrolyte additive enabled fast charging and stable cycling lithium metal batteries. *Nat. Energy.* **2017**, *2*, 17012. DOI
10. Chang, Z.; Qiao, Y.; Yang, H.; et al. Beyond the concentrated electrolyte: further depleting solvent molecules within a Li^+ solvation sheath to stabilize high-energy-density lithium metal batteries. *Energy. Environ. Sci.* **2020**, *13*, 4122-31. DOI
11. Lu, Y.; Tu, Z.; Archer, L. A. Stable lithium electrodeposition in liquid and nanoporous solid electrolytes. *Nat. Mater.* **2014**, *13*, 961-9. DOI PubMed
12. Wang, Z.; Tan, R.; Wang, H.; et al. A metal-organic-framework-based electrolyte with nanowetted interfaces for high-energy-density solid-state lithium battery. *Adv. Mater.* **2018**, *30*, 1704436. DOI
13. Chang, Z.; Yang, H.; Zhu, X.; He, P.; Zhou, H. A stable quasi-solid electrolyte improves the safe operation of highly efficient lithium-metal pouch cells in harsh environments. *Nat. Commun.* **2022**, *13*, 1510. DOI PubMed PMC
14. Furukawa, H.; Cordova, K. E.; O'Keeffe, M.; Yaghi, O. M. The chemistry and applications of metal-organic frameworks. *Science* **2013**, *341*, 1230444. DOI
15. Kitagawa, S.; Kitaura, R.; Noro, S. Functional porous coordination polymers. *Angew. Chem. Int. Ed.* **2004**, *43*, 2334-75. DOI PubMed
16. Cui, Y.; Li, B.; He, H.; Zhou, W.; Chen, B.; Qian, G. Metal-organic frameworks as platforms for functional materials. *Acc. Chem. Res.* **2016**, *49*, 483-93. DOI
17. Wang, L.; Han, Y.; Feng, X.; Zhou, J.; Qi, P.; Wang, B. Metal-organic frameworks for energy storage: batteries and supercapacitors. *Coord. Chem. Rev.* **2016**, *307*, 361-81. DOI
18. Yaghi, O. M.; Li, G.; Li, H. Selective binding and removal of guests in a microporous metal-organic framework. *Nature* **1995**, *378*, 703-6. DOI
19. Vaitsis, C.; Sourkouni, G.; Argirusis, C. Metal organic frameworks (MOFs) and ultrasound: a review. *Ultrason. Sonochem.* **2019**, *52*, 106-19. DOI PubMed
20. Lee, J.; Choi, I.; Kim, E.; Park, J.; Nam, K. W. Metal-organic frameworks for high-performance cathodes in batteries. *iScience* **2024**, *27*, 110211. DOI PubMed PMC
21. Zheng, Y.; Zheng, S.; Xue, H.; Pang, H. Metal-organic frameworks for lithium-sulfur batteries. *J. Mater. Chem. A.* **2019**, *7*, 3469-91. DOI
22. Chu, Z.; Gao, X.; Wang, C.; Wang, T.; Wang, G. Metal-organic frameworks as separators and electrolytes for lithium-sulfur batteries. *J. Mater. Chem. A.* **2021**, *9*, 7301-16. DOI
23. Chae, S.; Ko, M.; Kim, K.; Ahn, K.; Cho, J. Confronting issues of the practical implementation of Si anode in high-energy lithium-ion batteries. *Joule* **2017**, *1*, 47-60. DOI
24. Zhou, Y.; Long, J.; Li, Y. Ni-based catalysts derived from a metal-organic framework for selective oxidation of alkanes. *Chin. J. Catal.* **2016**, *37*, 955-62. DOI
25. Eddaoudi, M.; Moler, D. B.; Li, H.; et al. Modular chemistry: secondary building units as a basis for the design of highly porous and robust metal-organic carboxylate frameworks. *Acc. Chem. Res.* **2001**, *34*, 319-30. DOI
26. Sun, L.; Campbell, M. G.; Dincă, M. Electrically conductive porous metal-organic frameworks. *Angew. Chem. Int. Ed.* **2016**, *55*, 3566-79. DOI PubMed
27. Xie, Z.; Cao, B.; Yue, X.; et al. Metal organic frameworks-based cathode materials for advanced Li-S batteries: a comprehensive review. *Nano. Res.* **2024**, *17*, 2592-618. DOI
28. Ren, J.; Huang, Y.; Zhu, H.; et al. Recent progress on MOF-derived carbon materials for energy storage. *Carbon. Energy.* **2020**, *2*, 176-202. DOI
29. Babkova, T.; Kiefer, R.; Le, Q. B. Hybrid electrolyte based on PEO and ionic liquid with in situ produced and dispersed silica for sustainable solid-state battery. *Sustainability* **2024**, *16*, 1683. DOI
30. Yang, S.; Zhang, Z.; Lin, J.; et al. Recent progress in quasi/all-solid-state electrolytes for lithium-sulfur batteries. *Front. Energy. Res.* **2022**, *10*, 945003. DOI
31. Reinoso, D. M.; de, T. G. C.; Fernández-Ropero, A. J.; Levenfeld, B.; Várez, A. Advancements in quasi-solid-state Li batteries: a rigid hybrid electrolyte using LATP porous ceramic membrane and infiltrated ionic liquid. *ACS. Appl. Energy. Mater.* **2024**, *7*, 1527-38. DOI PubMed PMC
32. Xin, S.; You, Y.; Wang, S.; Gao, H.; Yin, Y.; Guo, Y. Solid-state lithium metal batteries promoted by nanotechnology: progress and prospects. *ACS. Energy. Lett.* **2017**, *2*, 1385-94. DOI
33. Zhou, D.; Shanmukaraj, D.; Tkacheva, A.; Armand, M.; Wang, G. Polymer electrolytes for lithium-based batteries: advances and prospects. *Chem* **2019**, *5*, 2326-52. DOI
34. Vineeth, S.; Soni, C. B.; Sungjemmenla; et al. A quasi-solid state polymer electrolyte for high-rate and long-life sodium-metal batteries. *J. Energy. Storage.* **2023**, *73*, 108780. DOI

35. Xu, K. Electrolytes and interphases in Li-ion batteries and beyond. *Chem. Rev.* **2014**, *114*, 11503-618. DOI PubMed
36. Nitta, N.; Wu, F.; Lee, J. T.; Yushin, G. Li-ion battery materials: present and future. *Mater. Today.* **2015**, *18*, 252-64. DOI
37. Zhang, X.; Cheng, X.; Chen, X.; Yan, C.; Zhang, Q. Fluoroethylene carbonate additives to render uniform Li deposits in lithium metal batteries. *Adv. Funct. Mater.* **2017**, *27*, 1605989. DOI
38. Manthiram, A. A reflection on lithium-ion battery cathode chemistry. *Nat. Commun.* **2020**, *11*, 1550. DOI PubMed PMC
39. Goodenough, J. B.; Kim, Y. Challenges for rechargeable Li batteries. *Chem. Mater.* **2010**, *22*, 587-603. DOI
40. Zhang, H.; Eshetu, G. G.; Judez, X.; Li, C.; Rodriguez-Martínez, L. M.; Armand, M. Electrolyte additives for lithium metal anodes and rechargeable lithium metal batteries: progress and perspectives. *Angew. Chem. Int. Ed.* **2018**, *57*, 15002-27. DOI PubMed
41. Cheng, X. B.; Zhang, R.; Zhao, C. Z.; Zhang, Q. Toward safe lithium metal anode in rechargeable batteries: a review. *Chem. Rev.* **2017**, *117*, 10403-73. DOI PubMed
42. Lin, D.; Liu, Y.; Cui, Y. Reviving the lithium metal anode for high-energy batteries. *Nat. Nanotechnol.* **2017**, *12*, 194-206. DOI PubMed
43. Lingappan, N.; Lee, W.; Passerini, S.; Pecht, M. A comprehensive review of separator membranes in lithium-ion batteries. *Renew. Sustain. Energy. Rev.* **2023**, *187*, 113726. DOI
44. Valverde, A.; Gonçalves, R.; Silva, M. M.; et al. Metal-organic framework based PVDF separators for high rate cycling lithium-ion batteries. *ACS. Appl. Energy. Mater.* **2020**, *3*, 11907-19. DOI
45. Zhao, R.; Liang, Z.; Zou, R.; Xu, Q. Metal-organic frameworks for batteries. *Joule* **2018**, *2*, 2235-59. DOI
46. Wang, H.; Dai, H. Strongly coupled inorganic-nano-carbon hybrid materials for energy storage. *Chem. Soc. Rev.* **2013**, *42*, 3088-113. DOI PubMed
47. Li, D.; Hu, H.; Chen, B.; Lai, W. Y. Advanced current collector materials for high-performance lithium metal anodes. *Small* **2022**, *18*, 2200010. DOI
48. Zhao, E.; Luo, S.; Hu, A.; et al. Rational design of an in-build quasi-solid-state electrolyte for high-performance lithium-ion batteries with the silicon-based anode. *Chem. Eng. J.* **2023**, *463*, 142306. DOI
49. Fang, L.; Sun, W.; Hou, W.; Mao, Y.; Wang, Z.; Sun, K. Quasi-solid-state polymer electrolyte based on highly concentrated LiTFSI complexing DMF for ambient-temperature rechargeable lithium batteries. *Ind. Eng. Chem. Res.* **2022**, *61*, 7971-81. DOI
50. Wang, P.; He, X.; Lv, Z.; et al. Light-driven polymer-based all-solid-state lithium-sulfur battery operating at room temperature. *Adv. Funct. Mater.* **2023**, *33*, 2211074. DOI
51. Manthiram, A.; Yu, X.; Wang, S. Lithium battery chemistries enabled by solid-state electrolytes. *Nat. Rev. Mater.* **2017**, *2*, 16103. DOI
52. Dunn, B.; Kamath, H.; Tarascon, J. M. Electrical energy storage for the grid: a battery of choices. *Science* **2011**, *334*, 928-35. DOI PubMed
53. Yao, X.; Huang, N.; Han, F.; et al. High-performance all-solid-state lithium-sulfur batteries enabled by amorphous sulfur-coated reduced graphene oxide cathodes. *Adv. Energy. Mater.* **2017**, *7*, 1602923. DOI
54. Xiao, Q.; Yang, J.; Wang, X.; et al. Carbon-based flexible self-supporting cathode for lithium-sulfur batteries: progress and perspective. *Carbon. Energy.* **2021**, *3*, 271-302. DOI
55. Zhai, Y.; Yang, G.; Zeng, Z.; et al. Composite hybrid quasi-solid electrolyte for high-energy lithium metal batteries. *ACS. Appl. Energy. Mater.* **2021**, *4*, 7973-82. DOI
56. Li, Z.; Weng, S.; Fu, J.; et al. Nonflammable quasi-solid electrolyte for energy-dense and long-cycling lithium metal batteries with high-voltage Ni-rich layered cathodes. *Energy. Storage. Mater.* **2022**, *47*, 542-50. DOI
57. Utpalla, P.; Mor, J.; Pujari, P. K.; Sharma, S. K. High ionic conductivity and ion conduction mechanism in ZIF-8 based quasi-solid-state electrolytes: a positron annihilation and broadband dielectric spectroscopy study. *Phys. Chem. Chem. Phys.* **2022**, *24*, 24999-5009. DOI PubMed
58. Zhang, W.; Li, S.; Zhang, Y.; Wang, X.; Liu, J.; Zheng, Y. A quasi-solid-state electrolyte with high ionic conductivity for stable lithium-ion batteries. *Sci. China. Technol. Sci.* **2022**, *65*, 2369-79. DOI
59. Yang, X.; Zhang, B.; Tian, Y.; et al. Electrolyte design principles for developing quasi-solid-state rechargeable halide-ion batteries. *Nat. Commun.* **2023**, *14*, 925. DOI PubMed PMC
60. Chen, Z.; Kim, G.; Kim, J.; et al. Highly stable quasi-solid-state lithium metal batteries: reinforced $Li_{1.3}Al_{0.3}Ti_{1.7}(PO_4)_3$/Li interface by a protection interlayer. *Adv. Energy. Mater.* **2021**, *11*, 2101339. DOI
61. Tian, R.; Jia, J.; Zhai, M.; et al. Design advanced lithium metal anode materials in high energy density lithium batteries. *Heliyon* **2024**, *10*, e27181. DOI PubMed PMC
62. Angarita-Gomez, S.; Balbuena, P. B. Insights into lithium ion deposition on lithium metal surfaces. *Phys. Chem. Chem. Phys.* **2020**, *22*, 21369-82. DOI PubMed
63. Zinth, V.; von, L. C.; Hofmann, M.; et al. Lithium plating in lithium-ion batteries at sub-ambient temperatures investigated by in situ neutron diffraction. *J. Power. Sources.* **2014**, *271*, 152-9. DOI
64. Koralalage, M. K.; Shreyas, V.; Arnold, W. R.; et al. Functionalization of cathode-electrolyte interface with ionic liquids for high-performance quasi-solid-state lithium-sulfur batteries: a low-sulfur loading study. *Batteries* **2024**, *10*, 155. DOI
65. Liang, S.; Yan, W.; Wu, X.; et al. Gel polymer electrolytes for lithium ion batteries: Fabrication, characterization and performance. *Solid. State. Ionics.* **2018**, *318*, 2-18. DOI
66. Li, W.; Li, H.; Liu, J.; et al. Systematic safety evaluation of quasi-solid-state lithium batteries: a case study. *Energy. Environ. Sci.*

2023, *16*, 5444-53. DOI

67. Liu, X.; Jia, H.; Li, H. Flame-retarding quasi-solid polymer electrolytes for high-safety lithium metal batteries. *Energy. Storage. Mater.* **2024**, *67*, 103263. DOI
68. Lim, D.; Jeong, B.; Kim, H.; et al. Safety enhanced quasi-solid-state electrolyte based on thiol-ene click chemistry for rechargeable lithium ion batteries. *Meet. Abstr.* **2021**, *MA2021-01*, 133. DOI
69. Lin, L.; Liu, F.; Zhang, Y.; et al. Adjustable mixed conductive interphase for dendrite-free lithium metal batteries. *ACS. Nano.* **2022**, *16*, 13101-10. DOI
70. Lu, X.; Wang, Y.; Xu, X.; Yan, B.; Wu, T.; Lu, L. Polymer-based solid-state electrolytes for high-energy-density lithium-ion batteries - review. *Adv. Energy. Mater.* **2023**, *13*, 2301746. DOI
71. Hu, H.; Li, J.; Ji, X. Confining ionic liquids in developing quasi-solid-state electrolytes for lithium metal batteries. *Chem. Eur. J.* **2024**, *30*, e202302826. DOI
72. Yu, D.; Tronstad, Z. C.; McCloskey, B. D. Lithium-ion transport and exchange between phases in a concentrated liquid electrolyte containing lithium-ion-conducting inorganic particles. *ACS. Energy. Lett.* **2024**, *9*, 1717-24. DOI PubMed PMC
73. Zhao, Y.; Song, Z.; Li, X.; et al. Metal organic frameworks for energy storage and conversion. *Energy. Storage. Mater.* **2016**, *2*, 35-62. DOI
74. Pan, K.; Zhang, L.; Qian, W.; et al. A flexible ceramic/polymer hybrid solid electrolyte for solid-state lithium metal batteries. *Adv. Mater.* **2020**, *32*, 2000399. DOI
75. Bao, H.; Chen, D.; Liao, B.; Yi, Y.; Liu, R.; Sun, Y. Enhanced ionic conduction in metal-organic-framework-based quasi-solid-state electrolytes: mechanistic insights. *Energy. Fuels.* **2024**, *38*, 11275-83. DOI
76. Kim, T.; Son, D.; Ono, L. K.; Jiang, Y.; Qi, Y. A solid-liquid hybrid electrolyte for lithium ion batteries enabled by a single-body polymer/indium tin oxide architecture. *J. Phys. D:. Appl. Phys.* **2021**, *54*, 475501. DOI
77. Wu, Z.; Yi, Y.; Hai, F.; et al. A metal-organic framework based quasi-solid-state electrolyte enabling continuous ion transport for high-safety and high-energy-density lithium metal batteries. *ACS. Appl. Mater. Interfaces.* **2023**, *15*, 22065-74. DOI
78. Han, D.; Zhao, Z.; Wang, W.; et al. Metal organic framework optimized hybrid solid polymer electrolytes with a high lithium-ion transference number and excellent electrochemical stability. *Sustain. Energy. Fuels.* **2022**, *6*, 4528-38. DOI
79. Dong, P.; Zhang, X.; Hiscox, W.; et al. Toward high-performance metal-organic-framework-based quasi-solid-state electrolytes: tunable structures and electrochemical properties. *Adv. Mater.* **2023**, *35*, e2211841. DOI
80. Li, J.; Weng, Z.; Qin, Z.; et al. Recent advances in multifunctional metal-organic frameworks for lithium metal batteries. *Sci. China. Chem.* **2024**, *67*, 759-73. DOI
81. Liu, W.; Mi, Y.; Weng, Z.; Zhong, Y.; Wu, Z.; Wang, H. Functional metal-organic framework boosting lithium metal anode performance via chemical interactions. *Chem. Sci.* **2017**, *8*, 4285-91. DOI
82. Zhang, Q.; Xiao, Y.; Li, Q.; et al. Design of thiol-lithium ion interaction in metal-organic framework for high-performance quasi-solid lithium metal batteries. *Dalton. Trans.* **2021**, *50*, 2928-35. DOI
83. Yang, H.; Wu, N. Ionic conductivity and ion transport mechanisms of solid-state lithium-ion battery electrolytes: a review. *Energy. Sci. Eng.* **2022**, *10*, 1643-71. DOI
84. Li, J.; Li, F.; Zhang, L.; Zhang, H.; Lassi, U.; Ji, X. Recent applications of ionic liquids in quasi-solid-state lithium metal batteries. *Green. Chem. Eng.* **2021**, *2*, 253-65. DOI
85. Luo, B.; Wang, Q.; Ji, W.; et al. Suppressing lithium dendrite via hybrid interface layers for high performance quasi-solid-state lithium metal batteries. *Chem. Eng. J.* **2024**, *492*, 152152. DOI
86. Zheng, B.; Zhu, J.; Wang, H.; et al. Stabilizing $Li_{10}SnP_2S_{12}$/Li interface via an in situ formed solid electrolyte interphase layer. *ACS. Appl. Mater. Interfaces.* **2018**, *10*, 25473-82. DOI
87. Wang, W.; Chai, M.; Lin, R.; et al. Amorphous MOFs for next generation supercapacitors and batteries. *Energy. Adv.* **2023**, *2*, 1591-603. DOI
88. Duan, S.; Qian, L.; Zheng, Y.; et al. Mechanisms of the accelerated Li^+ conduction in MOF-based solid-state polymer electrolytes for all-solid-state lithium metal batteries. *Adv. Mater.* **2024**, *36*, 2314120. DOI
89. Loo, K. L.; Ho, J. W.; Chung, C.; Moon, M.; Yoo, P. J. Ion-transporting channel-embedded MOF-in-COF structures as composite quasi-solid electrolytes with highly enhanced electrochemical properties. *J. Mater. Chem. A.* **2024**, *12*, 7875-85. DOI
90. Zhang, Z.; Tian, L.; Zhang, H.; et al. Hexagonal rodlike Cu-MOF-74-derived filler-reinforced composite polymer electrolyte for high-performance solid-state lithium batteries. *ACS. Appl. Energy. Mater.* **2022**, *5*, 1095-105. DOI
91. Miner, E. M.; Dincă, M. Metal- and covalent-organic frameworks as solid-state electrolytes for metal-ion batteries. *Phil. Trans. R. Soc. A.* **2019**, *377*, 20180225. DOI PubMed PMC
92. Hong, C. N.; Crom, A. B.; Feldblyum, J. I.; Lukatskaya, M. R. Metal-organic frameworks for fast electrochemical energy storage: mechanisms and opportunities. *Chem* **2023**, *9*, 798-822. DOI
93. Sun, R.; Dou, M.; Chen, Z.; et al. Engineering strategies of metal-organic frameworks toward advanced batteries. *Battery. Energy.* **2023**, *2*, 20220064. DOI
94. Yu, J.; Lin, L.; Cheng, L.; Wu, Q.; Zhao, L.; Wang, H. Engineering the interfacial compatibility of a small-molecule quinone cathode toward stable quasi-solid-state lithium-organic batteries. *ACS. Sustainable. Chem. Eng.* **2024**, *12*, 9969-77. DOI
95. Kim, M.; Çakmakçı, N.; Song, H.; Jeong, Y. Interfacially-enhanced quasi-solid electrolyte using ionic liquid for lithium-ion battery. *Mater. Res. Bull.* **2024**, *170*, 112588. DOI

96. Eftekhari, A. Lithium batteries for electric vehicles: from economy to research strategy. *ACS. Sustainable. Chem. Eng.* **2019**, *7*, 5602-13. DOI
97. Zhang, Q.; Liu, B.; Wang, J.; et al. The optimized interfacial compatibility of metal-organic frameworks enables a high-performance quasi-solid metal battery. *ACS. Energy. Lett.* **2020**, *5*, 2919-26. DOI
98. Wei, Y.; Hu, F.; Li, Y.; et al. Constructing stable anodic interphase for quasi-solid-state lithium-sulfur batteries. *ACS. Appl. Mater. Interfaces.* **2020**, *12*, 39335-41. DOI
99. Brus, J.; Czernek, J.; Urbanova, M.; Rohlíček, J.; Plecháček, T. Transferring lithium ions in the nanochannels of flexible metal-organic frameworks featuring superchaotropic metallacarborane guests: mechanism of ionic conductivity at atomic resolution. *ACS. Appl. Mater. Interfaces.* **2020**, *12*, 47447-56. DOI PubMed
100. Giacobbe, C.; Lavigna, E.; Maspero, A.; Galli, S. Elucidating the CO_2 adsorption mechanisms in the triangular channels of the bis(pyrazolate) MOF $Fe_2(BPEB)_3$ by in situ synchrotron X-ray diffraction and molecular dynamics simulations. *J. Mater. Chem. A.* **2017**, *5*, 16964-75. DOI
101. Hou, T.; Fong, K. D.; Wang, J.; Persson, K. A. Correction: the solvation structure, transport properties and reduction behavior of carbonate-based electrolytes of lithium-ion batteries. *Chem. Sci.* **2022**, *13*, 8205. DOI PubMed PMC
102. Xu, W.; Pei, X.; Diercks, C. S.; Lyu, H.; Ji, Z.; Yaghi, O. M. A metal-organic framework of organic vertices and polyoxometalate linkers as a solid-state electrolyte. *J. Am. Chem. Soc.* **2019**, *141*, 17522-6. DOI
103. Hou, T.; Xu, W.; Pei, X.; Jiang, L.; Yaghi, O. M.; Persson, K. A. Ionic conduction mechanism and design of metal-organic framework based quasi-solid-state electrolytes. *J. Am. Chem. Soc.* **2022**, *144*, 13446-50. DOI PubMed PMC
104. Su, N. C.; Noor, S. A. M.; Roslee, M. F.; Mohamed, N. S.; Ahmad, A.; Yahya, M. Z. A. Potential complexes of $NaCF_3SO_3$-tetraethylene dimethyl glycol ether (tetraglyme)-based electrolytes for sodium rechargeable battery application. *Ionics* **2019**, *25*, 541-9. DOI
105. Singh, H. P.; Kumar, R.; Sekhon, S. S. Correlation between ionic conductivity and fluidity of polymer gel electrolytes containing $NH4CF_3SO_3$. *Bull. Mater. Sci.* **2005**, *28*, 467-72. DOI
106. Castillo, J.; Santiago, A.; Judez, X.; et al. High energy density lithium-sulfur batteries based on carbonaceous two-dimensional additive cathodes. *ACS. Appl. Energy. Mater.* **2023**, *6*, 3579-89. DOI
107. Kwon, W. J.; Kim, H.; Jung, K.; et al. Enhanced Li^+ conduction in perovskite $Li_3xLa_{/3-}x\square_{1/3-2}xTiO_3$ solid-electrolytes via microstructural engineering. *J. Mater. Chem. A.* **2017**, *5*, 6257-62. DOI
108. Zhu, Y.; He, X.; Mo, Y. First principles study on electrochemical and chemical stability of solid electrolyte-electrode interfaces in all-solid-state Li-ion batteries. *J. Mater. Chem. A.* **2016**, *4*, 3253-66. DOI
109. Luo, W.; Gong, Y.; Zhu, Y.; et al. Reducing interfacial resistance between garnet-structured solid-state electrolyte and Li-metal anode by a germanium layer. *Adv. Mater.* **2017**, 29. DOI
110. Chen, L.; Li, Y.; Li, S.; Fan, L.; Nan, C.; Goodenough, J. B. PEO/garnet composite electrolytes for solid-state lithium batteries: from "ceramic-in-polymer" to "polymer-in-ceramic". *Nano. Energy.* **2018**, *46*, 176-84. DOI
111. Wan, J.; Xie, J.; Kong, X.; et al. Ultrathin, flexible, solid polymer composite electrolyte enabled with aligned nanoporous host for lithium batteries. *Nat. Nanotechnol.* **2019**, *14*, 705-11. DOI
112. Song, K.; Chen, W. An effective solid-electrolyte interphase for stable solid-state batteries. *Chem* **2021**, *7*, 3195-7. DOI
113. Zhou, W.; Wang, S.; Li, Y.; Xin, S.; Manthiram, A.; Goodenough, J. B. Plating a dendrite-free lithium anode with a polymer/ceramic/polymer sandwich electrolyte. *J. Am. Chem. Soc.* **2016**, *138*, 9385-8. DOI
114. Kim, S. Y.; Cha, H.; Kostecki, R.; Chen, G. Composite cathode design for high-energy all-solid-state lithium batteries with long cycle life. *ACS. Energy. Lett.* **2023**, *8*, 521-8. DOI
115. Zhou, B.; Fang, B.; Stosevski, I.; Bonakdarpour, A.; Wilkinson, D. P. Li host carbon materials as the negative electrode for a Li-metal battery - mechanistic and practical assessment. *Meet. Abstr.* **2022**, *MA2022-01*, 667. DOI
116. Zheng, Z.; Ye, H.; Guo, Z. Recent progress on pristine metal/covalent-organic frameworks and their composites for lithium-sulfur batteries. *Energy. Environ. Sci.* **2021**, *14*, 1835-53. DOI
117. Chen, Y.; Wen, K.; Chen, T.; Zhang, X.; Armand, M.; Chen, S. Recent progress in all-solid-state lithium batteries: The emerging strategies for advanced electrolytes and their interfaces. *Energy. Storage. Mater.* **2020**, *31*, 401-33. DOI
118. Chen, S.; Wen, K.; Fan, J.; Bando, Y.; Golberg, D. Progress and future prospects of high-voltage and high-safety electrolytes in advanced lithium batteries: from liquid to solid electrolytes. *J. Mater. Chem. A.* **2018**, *6*, 11631-63. DOI
119. Chen, R.; Qu, W.; Guo, X.; Li, L.; Wu, F. The pursuit of solid-state electrolytes for lithium batteries: from comprehensive insight to emerging horizons. *Mater. Horiz.* **2016**, *3*, 487-516. DOI
120. Ong, J. L.; Loy, A. C. M.; Teng, S. Y.; How, B. S. Future paradigm of 3D printed Ni-based metal organic framework catalysts for dry methane reforming: techno-economic and environmental analyses. *ACS. Omega.* **2022**, *7*, 15369-84. DOI PubMed PMC
121. Desantis, D.; Mason, J. A.; James, B. D.; Houchins, C.; Long, J. R.; Veenstra, M. Techno-economic analysis of metal-organic frameworks for hydrogen and natural gas storage. *Energy. Fuels.* **2017**, *31*, 2024-32. DOI
122. Paul, T.; Juma, A.; Alqerem, R.; Karanikolos, G.; Arafat, H. A.; Dumée, L. F. Scale-up of metal-organic frameworks production: engineering strategies and prospects towards sustainable manufacturing. *J. Environ. Chem. Eng.* **2023**, *11*, 111112. DOI
123. Chakraborty, D.; Yurdusen, A.; Mouchaham, G.; Nouar, F.; Serre, C. Large-scale production of metal-organic frameworks. *Adv. Funct. Mater.* **2024**, *34*, 2309089. DOI
124. Yusuf, V. F.; Malek, N. I.; Kailasa, S. K. Review on metal-organic framework classification, synthetic approaches, and influencing

factors: applications in energy, drug delivery, and wastewater treatment. *ACS. Omega.* **2022**, *7*, 44507-31. DOI PubMed PMC

125. Sun, C.; Liu, J.; Gong, Y.; Wilkinson, D. P.; Zhang, J. Recent advances in all-solid-state rechargeable lithium batteries. *Nano. Energy.* **2017**, *33*, 363-86. DOI
126. Han, X.; Gong, Y.; Fu, K. K.; et al. Negating interfacial impedance in garnet-based solid-state Li metal batteries. *Nat. Mater.* **2017**, *16*, 572-9. DOI
127. Wang, C.; Fu, K.; Kammampata, S. P.; et al. Garnet-type solid-state electrolytes: materials, interfaces, and batteries. *Chem. Rev.* **2020**, *120*, 4257-300. DOI
128. Kaur, G.; Sharma, S.; Singh, M. D.; Nalwa, K. S.; Sivasubramanian, S. C.; Dalvi, A. Ionic liquid composites with garnet-type $Li_{6.75}Al_{0.25}La_3Zr_2O_{12}$: stability, electrical transport, and potential for energy storage applications. *Mater. Chem. Phys.* **2024**, *317*, 129205. DOI
129. Zhang, Z.; Zhang, L.; Liu, Y.; et al. Interface-engineered $Li_7La_3Zr_2O_{12}$-based garnet solid electrolytes with suppressed li-dendrite formation and enhanced electrochemical performance. *ChemSusChem* **2018**, *11*, 3774-82. DOI
130. Lin, R.; Jin, Y.; Li, Y.; Zhang, X.; Xiong, Y. Recent advances in ionic liquids-MOF hybrid electrolytes for solid-state electrolyte of lithium battery. *Batteries* **2023**, *9*, 314. DOI
131. Subramani, R.; Hsu, S.; Chuang, Y.; Hsu, L.; Lu, K.; Chen, J. Fe-MIL-101 metal organic framework integrated solid polymer electrolytes for high-performance solid-state lithium metal batteries. *J. Mater. Chem. A.* **2024**, *12*, 7132-41. DOI
132. Homann, G.; Stolz, L.; Nair, J.; Laskovic, I. C.; Winter, M.; Kasnatscheew, J. Poly(ethylene oxide)-based electrolyte for solid-state-lithium-batteries with high voltage positive electrodes: evaluating the role of electrolyte oxidation in rapid cell failure. *Sci. Rep.* **2020**, *10*, 4390. DOI PubMed PMC
133. Wang, Q.; Yang, A.; Ma, J.; Yao, M.; Geng, S.; Liu, F. Constructing PTFE@LATP composite solid electrolytes with three-dimensional network for high-performance lithium batteries. *Electrochim. Acta.* **2023**, *467*, 143138. DOI
134. Liu, Y.; Xu, Y.; Zhang, Y.; Yu, C.; Sun, X. Thin $Li_{1.3}Al_{0.3}Ti_{1.7}(PO_4)_3$-based composite solid electrolyte with a reinforced interface of in situ formed poly(1,3-dioxolane) for lithium metal batteries. *J. Colloid. Interface. Sci.* **2023**, *644*, 53-63. DOI
135. Xu, Y.; Zhao, R.; Gao, L.; et al. A fiber-reinforced solid polymer electrolyte by in situ polymerization for stable lithium metal batteries. *Nano. Res.* **2023**, *16*, 9259-66. DOI
136. Butreddy, P.; Wijesingha, M.; Laws, S.; Pathiraja, G.; Mo, Y.; Rathnayake, H. Insight into the isoreticularity of Li-MOFs for the design of low-density solid and quasi-solid electrolytes. *Chem. Mater.* **2023**, *35*, 9857-78. DOI PubMed PMC
137. Gong, X.; Xiao, Q.; Li, Q.; et al. Cross-linked electrospun gel polymer electrolytes for lithium-ion batteries. *Chin. J. Polym. Sci.* **2024**, *42*, 1021-8. DOI
138. Lim, N.; Kim, E.; Park, J.; et al. Design of a bioinspired robust three-dimensional cross-linked polymer binder for high-performance Li-ion battery applications. *ACS. Appl. Mater. Interfaces.* **2023**, *15*, 54409-18. DOI
139. Shin, W.; Cho, J.; Kannan, A. G.; Lee, Y.; Kim, D. Cross-linked composite gel polymer electrolyte using mesoporous methacrylate-functionalized SiO_2 nanoparticles for lithium-ion polymer batteries. *Sci. Rep.* **2016**, *6*, BFsrep26332. DOI PubMed PMC
140. Röchow, E. T.; Coeler, M.; Pospiech, D.; et al. In situ preparation of crosslinked polymer electrolytes for lithium ion batteries: a comparison of monomer systems. *Polymers* **2020**, *12*, 1707. DOI PubMed PMC
141. Wen, J.; Zhao, Q.; Jiang, X.; et al. Graphene oxide enabled flexible peo-based solid polymer electrolyte for all-solid-state lithium metal battery. *ACS. Appl. Energy. Mater.* **2021**, *4*, 3660-9. DOI
142. Rajamani, A.; Panneerselvam, T.; Murugan, R.; Ramaswamy, A. P. Electrospun derived polymer-garnet composite quasi solid state electrolyte with low interface resistance for lithium metal batteries. *Energy* **2023**, *263*, 126058. DOI
143. Huang, Y.; Wang, Y.; Fu, Y. A thermoregulating separator based on black phosphorus/MOFs heterostructure for thermo-stable lithium-sulfur batteries. *Chem. Eng. J.* **2023**, *454*, 140250. DOI
144. Lei, H.; Tu, J.; Li, S.; et al. MOF-based quasi-solid-state electrolyte for long-life Al-Se battery. *J. Energy. Chem.* **2023**, *86*, 237-45. DOI
145. Zhang, Z.; Huang, Y.; Li, C.; Li, X. Metal-organic framework-supported poly(ethylene oxide) composite gel polymer electrolytes for high-performance lithium/sodium metal batteries. *ACS. Appl. Mater. Interfaces.* **2021**, *13*, 37262-72. DOI
146. Li, J.; Gao, L.; Pan, F.; et al. Engineering strategies for suppressing the shuttle effect in lithium-sulfur batteries. *Nano-Micro. Lett.* **2023**, *16*, 12. DOI
147. Aslam, M. K.; Niu, Y.; Hussain, T.; et al. How to avoid dendrite formation in metal batteries: innovative strategies for dendrite suppression. *Nano. Energy.* **2021**, *86*, 106142. DOI
148. Bai, S.; Kim, B.; Kim, C.; et al. Permselective metal-organic framework gel membrane enables long-life cycling of rechargeable organic batteries. *Nat. Nanotechnol.* **2021**, *16*, 77-84. DOI
149. Liu, Q.; Yang, L.; Mei, Z.; et al. Constructing host-guest recognition electrolytes promotes the Li^+ kinetics in solid-state batteries. *Energy. Environ. Sci.* **2024**, *17*, 780-90. DOI
150. Yang, L.; Chen, J.; Park, S.; Wang, H. Recent progress on metal-organic framework derived carbon and their composites as anode materials for potassium-ion batteries. *Energy. Mater.* **2023**, *3*, 300042. DOI
151. Chen, J.; Adit, G.; Li, L.; Zhang, Y.; Chua, D. H. C.; Lee, P. S. Optimization strategies toward functional sodium-ion batteries. *Energy. Environ. Mater.* **2023**, *6*, e12633. DOI
152. Lu, X.; Wu, H.; Kong, D.; Li, X.; Shen, L.; Lu, Y. Facilitating lithium-ion conduction in gel polymer electrolyte by metal-organic frameworks. *ACS. Mater. Lett.* **2020**, *2*, 1435-41. DOI

153. Fu, X.; Hurlock, M. J.; Ding, C.; Li, X.; Zhang, Q.; Zhong, W. H. MOF-enabled ion-regulating gel electrolyte for long-cycling lithium metal batteries under high voltage. *Small* **2022**, *18*, 2106225. DOI
154. Wang, D.; Jin, B.; Yao, X.; et al. Bio-inspired polydopamine-modified ZIF-90-supported gel polymer electrolyte for high-safety lithium metal batteries. *ACS. Appl. Energy. Mater.* **2023**, *6*, 11146-56. DOI
155. Murray, L. J.; Dincă, M.; Long, J. R. Hydrogen storage in metal-organic frameworks. *Chem. Soc. Rev.* **2009**, *38*, 1294-314. DOI PubMed
156. Li, J. R.; Sculley, J.; Zhou, H. C. Metal-organic frameworks for separations. *Chem. Rev.* **2012**, *112*, 869-932. DOI PubMed
157. Ma, L.; Abney, C.; Lin, W. Enantioselective catalysis with homochiral metal-organic frameworks. *Chem. Soc. Rev.* **2009**, *38*, 1248-56. DOI PubMed
158. Kreno, L. E.; Leong, K.; Farha, O. K.; Allendorf, M.; Van, D. R. P.; Hupp, J. T. Metal-organic framework materials as chemical sensors. *Chem. Rev.* **2012**, *112*, 1105-25. DOI PubMed
159. Min, K. S.; Suh, M. P. Silver(I)-polynitrile network solids for anion exchange: anion-induced transformation of supramolecular structure in the crystalline state. *J. Am. Chem. Soc.* **2000**, *122*, 6834-40. DOI
160. Horike, S.; Umeyama, D.; Kitagawa, S. Ion conductivity and transport by porous coordination polymers and metal-organic frameworks. *Acc. Chem. Res.* **2013**, *46*, 2376-84. DOI PubMed
161. Yang, H.; Liu, B.; Bright, J.; et al. A single-ion conducting UiO-66 metal-organic framework electrolyte for all-solid-state lithium batteries. *ACS. Appl. Energy. Mater.* **2020**, *3*, 4007-13. DOI
162. Liu, X. Metal-organic framework UiO-66 membranes. *Front. Chem. Sci. Eng.* **2020**, *14*, 216-32. DOI
163. Taylor, J. M.; Dekura, S.; Ikeda, R.; Kitagawa, H. Defect control to enhance proton conductivity in a metal-organic framework. *Chem. Mater.* **2015**, *27*, 2286-9. DOI
164. Chen, X.; Li, G. Proton conductive Zr-based MOFs. *Inorg. Chem. Front.* **2020**, *7*, 3765-84. DOI
165. Liu, L.; Sun, C. Flexible quasi-solid-state composite electrolyte membrane derived from a metal-organic framework for lithium-metal batteries. *ChemElectroChem* **2020**, *7*, 707-15. DOI
166. Zhou, L.; Pan, H.; Yin, G.; et al. Tailoring the function of battery separators via the design of MOF coatings. *Adv. Funct. Mater.* **2024**, *34*, 2314246. DOI
167. Wu, X.; Gao, Y.; Bi, J. Understanding the structure-dependent adsorption behavior of four zirconium-based porphyrinic MOFs for the removal of pharmaceuticals. *Microporous. Mesoporous. Mater.* **2024**, *363*, 112827. DOI
168. Furukawa, H.; Gándara, F.; Zhang, Y. B.; et al. Water adsorption in porous metal-organic frameworks and related materials. *J. Am. Chem. Soc.* **2014**, *136*, 4369-81. DOI
169. Sun, C.; Zhang, J. H.; Yuan, X. F.; et al. ZIF-8-based quasi-solid-state electrolyte for lithium batteries. *ACS. Appl. Mater. Interfaces.* **2019**, *11*, 46671-7. DOI
170. Zhu, X.; Chang, Z.; Yang, H.; He, P.; Zhou, H. Highly safe and stable lithium-metal batteries based on a quasi-solid-state electrolyte. *J. Mater. Chem. A.* **2022**, *10*, 651-63. DOI
171. Shieh, F. K.; Wang, S. C.; Leo, S. Y.; Wu, K. C. Water-based synthesis of zeolitic imidazolate framework-90 (ZIF-90) with a controllable particle size. *Chem. Eur. J.* **2013**, *19*, 11139-42. DOI PubMed
172. Kida, K.; Okita, M.; Fujita, K.; Tanaka, S.; Miyake, Y. Formation of high crystalline ZIF-8 in an aqueous solution. *CrystEngComm* **2013**, *15*, 1794-801. DOI
173. Yu, T.; Ma, H.; Zhang, H.; Xiong, M.; Liu, Y.; Li, F. Fabrication and characterization of purified esterase-embedded zeolitic imidazolate frameworks for the removal and remediation of herbicide pollution from soil. *J. Environ. Manage.* **2021**, *288*, 112450. DOI
174. Deneff, J. I.; Butler, K. S.; Kotula, P. G.; Rue, B. E.; Sava, G. D. F. Expanding the ZIFs repertoire for biological applications with the targeted synthesis of ZIF-20 nanoparticles. *ACS. Appl. Mater. Interfaces.* **2021**, *13*, 27295-304. DOI PubMed
175. Xing, J.; Schweighauser, L.; Okada, S.; Harano, K.; Nakamura, E. Atomistic structures and dynamics of prenucleation clusters in MOF-2 and MOF-5 syntheses. *Nat. Commun.* **2019**, *10*, 3608. DOI PubMed PMC
176. Xu, G.; Yamada, T.; Otsubo, K.; Sakaida, S.; Kitagawa, H. Facile "modular assembly" for fast construction of a highly oriented crystalline MOF nanofilm. *J. Am. Chem. Soc.* **2012**, *134*, 16524-7. DOI PubMed
177. Shen, L.; Wu, H. B.; Liu, F.; et al. Creating lithium-ion electrolytes with biomimetic ionic channels in metal-organic frameworks. *Adv. Mater.* **2018**, *30*, 1707476. DOI
178. Wang, X. G.; Cheng, Q.; Yu, Y.; Zhang, X. Z. Controlled nucleation and controlled growth for size predicable synthesis of nanoscale metal-organic frameworks (MOFs): a general and scalable approach. *Angew. Chem. Int. Ed.* **2018**, *57*, 7836-40. DOI
179. Qiu, S.; Du, J.; Xiao, Y.; Zhao, Q.; He, G. Hierarchical porous HKUST-1 fabricated by microwave-assisted synthesis with CTAB for enhanced adsorptive removal of benzothiophene from fuel. *Sep. Purif. Technol.* **2021**, *271*, 118868. DOI
180. Chen, Y.; Qiao, Z.; Lv, D.; et al. Efficient adsorptive separation of C_3H_6 over C_3H_8 on flexible and thermoresponsive CPL-1. *Chem. Eng. J.* **2017**, *328*, 360-7. DOI
181. Xiang, H.; Ameen, A.; Shang, J.; et al. Synthesis and modification of moisture-stable coordination pillared-layer metal-organic framework (CPL-MOF) CPL-2 for ethylene/ethane separation. *Microporous. Mesoporous. Mater.* **2020**, *293*, 109784. DOI
182. Garai, B.; Bon, V.; Krause, S.; et al. Tunable flexibility and porosity of the metal-organic framework DUT-49 through postsynthetic metal exchange. *Chem. Mater.* **2020**, *32*, 889-96. DOI
183. Kolbe, F.; Krause, S.; Bon, V.; Senkovska, I.; Kaskel, S.; Brunner, E. High-pressure in situ ^{129}Xe NMR spectroscopy: insights into

switching mechanisms of flexible metal-organic frameworks isoreticular to DUT-49. *Chem. Mater.* **2019**, *31*, 6193-201. DOI PubMed PMC

184. Wang, C.; Zhang, F.; Yang, J.; Li, J. Rapid and HF-free synthesis of MIL-100(Cr) via steam-assisted method. *Mater. Lett.* **2019**, *252*, 286-8. DOI
185. Celeste, A.; Paolone, A.; Itié, J. P.; et al. Mesoporous metal-organic framework MIL-101 at high pressure. *J. Am. Chem. Soc.* **2020**, *142*, 15012-9. DOI
186. Hu, J.; Chen, Y.; Zhang, H.; Chen, Z. Controlled syntheses of Mg-MOF-74 nanorods for drug delivery. *J. Solid. State. Chem.* **2021**, *294*, 121853. DOI
187. Qi, C.; Xu, L.; Wang, J.; et al. Titanium-containing metal-organic framework modified separator for advanced lithium-sulfur batteries. *ACS. Sustainable. Chem. Eng.* **2020**, *8*, 12968-75. DOI
188. Wang, Z.; Li, Z.; Zhang, X. G.; et al. Tailoring multiple sites of metal-organic frameworks for highly efficient and reversible ammonia adsorption. *ACS. Appl. Mater. Interfaces.* **2021**, *13*, 56025-34. DOI
189. Su, Y.; Yuan, G.; Hu, J.; et al. Thiosalicylic-acid-mediated coordination structure of nickel center via thermodynamic modulation for aqueous Ni-Zn batteries. *Adv. Mater.* **2024**, *36*, 2406094. DOI
190. Leng, X.; Zeng, J.; Yang, M.; et al. Bimetallic Ni-Co MOF@PAN modified electrospun separator enhances high-performance lithium-sulfur batteries. *J. Energy. Chem.* **2023**, *82*, 484-96. DOI
191. Razaq, R.; Din, M. M. U.; Småbråten, D. R.; et al. Synergistic effect of bimetallic MOF modified separator for long cycle life lithium-sulfur batteries. *Adv. Energy. Mater.* **2024**, *14*, 2302897. DOI
192. Liu, Y.; Li, L.; Wen, A.; Cao, F.; Ye, H. A Janus MXene/MOF separator for the all-in-one enhancement of lithium-sulfur batteries. *Energy. Storage. Mater.* **2023**, *55*, 652-9. DOI
193. Han, D. D.; Wang, Z. Y.; Pan, G. L.; Gao, X. P. Metal-organic-framework-based gel polymer electrolyte with immobilized anions to stabilize a lithium anode for a quasi-solid-state lithium-sulfur battery. *ACS. Appl. Mater. Interfaces.* **2019**, *11*, 18427-35. DOI PubMed
194. Férey, G.; Mellot-Draznieks, C.; Serre, C.; et al. A chromium terephthalate-based solid with unusually large pore volumes and surface area. *Science* **2005**, *309*, 2040-2. DOI
195. Xu, Z.; Zhao, Y. Y.; Chen, L.; et al. Thermally activated bipyridyl-based Mn-MOFs with Lewis acid-base bifunctional sites for highly efficient catalytic cycloaddition of CO_2 with epoxides and Knoevenagel condensation reactions. *Dalton. Trans.* **2023**, *52*, 3671-81. DOI
196. Zhang, X.; Zhan, Z.; Li, Z.; Di, L. Thermal activation of CuBTC MOF for CO oxidation: the effect of activation atmosphere. *Catalysts* **2017**, *7*, 106. DOI
197. He, Z.; Zhu, X.; Song, Y.; et al. Separator functionalization realizing stable zinc anode through microporous metal-organic framework with special functional group. *Energy. Storage. Mater.* **2025**, *74*, 103886. DOI
198. Planchais, A.; Devautour-vinot, S.; Salles, F.; et al. A joint experimental/computational exploration of the dynamics of confined water/Zr-based MOFs systems. *J. Phys. Chem. C.* **2014**, *118*, 14441-8. DOI
199. Yang, P.; Zhang, K.; Liu, S.; et al. Ionic selective separator design enables long-life zinc-iodine batteries via synergistic anode stabilization and polyiodide shuttle suppression. *Adv. Funct. Mater.* **2024**, *34*, 2410712. DOI
200. Ruan, Z.; Wang, X.; Yuan, X. Improved catalytic performance and stability of defected UiO-66-SO_3H in the esterification reaction of cyclohexene with cyclohexanecarboxylic acid. *J. Porous. Mater.* **2022**, *29*, 1957-68. DOI
201. Morris, W.; Volosskiy, B.; Demir, S.; et al. Synthesis, structure, and metalation of two new highly porous zirconium metal-organic frameworks. *Inorg. Chem.* **2012**, *51*, 6443-5. DOI
202. Kim, H. K.; Yun, W. S.; Kim, M. B.; et al. A chemical route to activation of open metal sites in the copper-based metal-organic framework materials HKUST-1 and Cu-MOF-2. *J. Am. Chem. Soc.* **2015**, *137*, 10009-15. DOI
203. Li, H.; Eddaoudi, M.; O'keeffe, M.; Yaghi, O. M. Design and synthesis of an exceptionally stable and highly porous metal-organic framework. *Nature* **1999**, *402*, 276-9. DOI
204. Liu, J.; Culp, J. T.; Natesakhawat, S.; et al. Experimental and theoretical studies of gas adsorption in $Cu_3(BTC)_2$: an effective activation procedure. *J. Phys. Chem. C.* **2007**, *111*, 9305-13. DOI
205. Lohe, M. R.; Rose, M.; Kaskel, S. Metal-organic framework (MOF) aerogels with high micro- and macroporosity. *Chem. Commun.* **2009**, 6056-8. DOI PubMed
206. Nelson, A. P.; Farha, O. K.; Mulfort, K. L.; Hupp, J. T. Supercritical processing as a route to high internal surface areas and permanent microporosity in metal-organic framework materials. *J. Am. Chem. Soc.* **2009**, *131*, 458-60. DOI PubMed
207. Mondloch, J. E.; Karagiaridi, O.; Farha, O. K.; Hupp, J. T. Activation of metal-organic framework materials. *CrystEngComm* **2013**, *15*, 9258. DOI
208. Oh, H.; Maurer, S.; Balderas-xicohtencatl, R.; et al. Efficient synthesis for large-scale production and characterization for hydrogen storage of ligand exchanged MOF-74/174/184-M (M = Mg^{2+}, Ni^{2}+). *Int. J. Hydrogen. Energy.* **2017**, *42*, 1027-35. DOI
209. Batten, M. P.; Rubio-martinez, M.; Hadley, T.; et al. Continuous flow production of metal-organic frameworks. *Curr. Opin. Chem. Eng.* **2015**, *8*, 55-9. DOI
210. Rubio-Martinez, M.; Avci-Camur, C.; Thornton, A. W.; Imaz, I.; Maspoch, D.; Hill, M. R. New synthetic routes towards MOF production at scale. *Chem. Soc. Rev.* **2017**, *46*, 3453-80. DOI PubMed
211. Gaab, M.; Trukhan, N.; Maurer, S.; Gummaraju, R.; Müller, U. The progression of Al-based metal-organic frameworks-from

academic research to industrial production and applications. *Microporous. Mesoporous. Mater.* **2012**, *157*, 131-6. DOI

212. Vepsäläinen, M.; Macedo, D. S.; Gong, H.; Rubio-martinez, M.; Bayatsarmadi, B.; He, B. Electrosynthesis of HKUST-1 with flow-reactor post-processing. *Appl. Sci.* **2021**, *11*, 3340. DOI
213. Ren, J.; Dyosiba, X.; Musyoka, N. M.; Langmi, H. W.; Mathe, M.; Liao, S. Review on the current practices and efforts towards pilot-scale production of metal-organic frameworks (MOFs). *Coord. Chem. Rev.* **2017**, *352*, 187-219. DOI
214. Mckinstry, C.; Cathcart, R. J.; Cussen, E. J.; Fletcher, A. J.; Patwardhan, S. V.; Sefcik, J. Scalable continuous solvothermal synthesis of metal organic framework (MOF-5) crystals. *Chem. Eng. J.* **2016**, *285*, 718-25. DOI
215. Klimakow, M.; Klobes, P.; Thünemann, A. F.; Rademann, K.; Emmerling, F. Mechanochemical synthesis of metal-organic frameworks: a fast and facile approach toward quantitative yields and high specific surface areas. *Chem. Mater.* **2010**, *22*, 5216-21. DOI
216. Tanaka, S.; Kida, K.; Nagaoka, T.; Ota, T.; Miyake, Y. Mechanochemical dry conversion of zinc oxide to zeolitic imidazolate framework. *Chem. Commun.* **2013**, *49*, 7884-6. DOI PubMed
217. Chen, Z.; Wang, W.; Yao, J.; et al. Toxicity of a molluscicide candidate PPU07 against Oncomelania hupensis (Gredler, 1881) and local fish in field evaluation. *Chemosphere* **2019**, *222*, 56-61. DOI
218. Cadot, S.; Veyre, L.; Luneau, D.; Farrusseng, D.; Alessandra, Q. E. A water-based and high space-time yield synthetic route to MOF Ni_2(dhtp) and its linker 2,5-dihydroxyterephthalic acid. *J. Mater. Chem. A.* **2014**, *2*, 17757-63. DOI
219. Sánchez, L.; Acevedo-peña, P.; Aguilar-frutis, M. Á.; Reguera, E. Improving Mg^{2+} ionic conductivity in ZIF-8 by Cu (II) doping and mbIm incorporation into the framework. *Solid. State. Ionics.* **2024**, *407*, 116497. DOI
220. Mu, A. U.; Cai, G.; Chen, Z. Metal-organic frameworks for the enhancement of lithium-based batteries: a mini review on emerging functional designs. *Adv. Sci.* **2024**, *11*, 2305280. DOI PubMed PMC
221. Zhang, M.; Wu, L.; Zhu, B.; Liu, Y. Performance enhancement of lithium-metal batteries using the three-dimensional porous network structure a metal-organic framework-aramid cellulose-MXene composite separator. *Int. J. Hydrogen. Energy.* **2024**, *59*, 263-71. DOI
222. Shang, W.; Chen, Y.; Han, J.; Ouyang, P.; Fang, C.; Du, J. Dendrite-free Li anode enabled by a metal-organic framework-modified solid polymer electrolyte for high-performance lithium metal batteries. *ACS. Appl. Energy. Mater.* **2020**, *3*, 12351-9. DOI
223. Wang, Z.; Du, Z.; Liu, Y.; et al. Metal-organic frameworks and their derivatives for optimizing lithium metal anodes. *eScience* **2024**, *4*, 100189. DOI
224. Lee, D. J.; Yu, X.; Sikma, R. E.; et al. Holistic design consideration of metal-organic framework-based composite membranes for lithium-sulfur batteries. *ACS. Appl. Mater. Interfaces.* **2022**, *14*, 34742-9. DOI
225. Phung, J.; Zhang, X.; Deng, W.; Li, G. An overview of MOF-based separators for lithium-sulfur batteries. *Sustain. Mater. Technol.* **2022**, *31*, e00374. DOI
226. Peng, Y.; Xu, J.; Xu, J.; et al. Metal-organic framework (MOF) composites as promising materials for energy storage applications. *Adv. Colloid. Interface. Sci.* **2022**, *307*, 102732. DOI
227. Bai, S.; Liu, X.; Zhu, K.; Wu, S.; Zhou, H. Metal-organic framework-based separator for lithium-sulfur batteries. *Nat. Energy.* **2016**, *1*, 16094. DOI
228. Li, Y. W.; Zhang, W. J.; Li, J.; et al. Fe-MOF-derived efficient ORR/OER bifunctional electrocatalyst for rechargeable zinc-air batteries. *ACS. Appl. Mater. Interfaces.* **2020**, *12*, 44710-9. DOI
229. He, J.; Chen, Y.; Manthiram, A. Vertical Co_9S_8 hollow nanowall arrays grown on a Celgard separator as a multifunctional polysulfide barrier for high-performance Li-S batteries. *Energy. Environ. Sci.* **2018**, *11*, 2560-8. DOI
230. Li, X.; Zhang, F.; Zhang, M.; Zhou, Z.; Zhou, X. Chromium-based metal-organic framework coated separator for improving electrochemical performance and safety of lithium-ion battery. *J. Energy. Storage.* **2023**, *59*, 106473. DOI
231. Chang, Z.; Qiao, Y.; Deng, H.; Yang, H.; He, P.; Zhou, H. A liquid electrolyte with de-solvated lithium ions for lithium-metal battery. *Joule* **2020**, *4*, 1776-89. DOI
232. Sheng, L.; Wang, Q.; Liu, X.; et al. Suppressing electrolyte-lithium metal reactivity via Li^+-desolvation in uniform nano-porous separator. *Nat. Commun.* **2022**, *13*, 172. DOI PubMed PMC
233. Hu, Q.; Han, G.; Wang, A.; et al. Functionalized MOF enables stable cycling of nickel-rich layered oxides for lithium-ion batteries. *Chem. Eng. J.* **2024**, *497*, 154608. DOI
234. Chang, Z.; Yang, H.; Pan, A.; He, P.; Zhou, H. An improved 9 micron thick separator for a 350 Wh/kg lithium metal rechargeable pouch cell. *Nat. Commun.* **2022**, *13*, 6788. DOI PubMed PMC
235. Fan, Y.; Niu, Z.; Zhang, F.; Zhang, R.; Zhao, Y.; Lu, G. Suppressing the shuttle effect in lithium-sulfur batteries by a UiO-66-modified polypropylene separator. *ACS. Omega.* **2019**, *4*, 10328-35. DOI
236. Han, J.; Gao, S.; Wang, R.; et al. Investigation of the mechanism of metal-organic frameworks preventing polysulfide shuttling from the perspective of composition and structure. *J. Mater. Chem. A.* **2020**, *8*, 6661-9. DOI
237. Zhu, F.; Bao, H.; Wu, X.; et al. High-performance metal-organic framework-based single ion conducting solid-state electrolytes for low-temperature lithium metal batteries. *ACS. Appl. Mater. Interfaces.* **2019**, *11*, 43206-13. DOI
238. Fan, Z.; He, L.; Li, X.; Xin, X. Inhibiting I^-/I_3^- redox shuttling in Li-O_2 batteries by MOF decorated separator. *Mater. Res. Bull.* **2023**, *167*, 112412. DOI
239. Aubrey, M. L.; Ameloot, R.; Wiers, B. M.; Long, J. R. Metal-organic frameworks as solid magnesium electrolytes. *Energy. Environ. Sci.* **2014**, *7*, 667-71. DOI
240. Ameloot, R.; Aubrey, M.; Wiers, B. M.; et al. Ionic conductivity in the metal-organic framework UiO-66 by dehydration and

insertion of lithium tert-butoxide. *Chemistry* **2013**, *19*, 5533-6. DOI

241. Zettl, R.; Lunghammer, S.; Gadermaier, B.; et al. High Li^+ and Na^+ conductivity in new hybrid solid electrolytes based on the porous MIL-121 metal organic framework. *Adv. Energy. Mater.* **2021**, *11*, 2003542. DOI
242. Lu, G.; Wei, H.; Shen, C.; et al. Bifunctional MOF doped PEO composite electrolyte for long-life cycle solid lithium ion battery. *ACS. Appl. Mater. Interfaces.* **2022**, *14*, 45476-83. DOI
243. Guo, Y.; Sun, M.; Liang, H.; et al. Blocking polysulfides and facilitating lithium-ion transport: polystyrene sulfonate@HKUST-1 membrane for lithium-sulfur batteries. *ACS. Appl. Mater. Interfaces.* **2018**, *10*, 30451-9. DOI
244. Kim, S. H.; Yeon, J. S.; Kim, R.; Choi, K. M.; Park, H. S. A functional separator coated with sulfonated metal-organic framework/Nafion hybrids for Li-S batteries. *J. Mater. Chem. A.* **2018**, *6*, 24971-8. DOI
245. Chang, Z.; Qiao, Y.; Wang, J.; Deng, H.; He, P.; Zhou, H. Fabricating better metal-organic frameworks separators for Li-S batteries: pore sizes effects inspired channel modification strategy. *Energy. Storage. Mater.* **2020**, *25*, 164-71. DOI
246. Wang, Z.; Huang, W.; Hua, J.; et al. An anionic-MOF-based bifunctional separator for regulating lithium deposition and suppressing polysulfides shuttle in Li-S batteries. *Small. Methods.* **2020**, *4*, 2000082. DOI
247. Zhou, Z.; Li, Y.; Fang, T.; et al. MOF-derived Co_3O_4 polyhedrons as efficient polysulfides barrier on polyimide separators for high temperature lithium-sulfur batteries. *Nanomaterials* **2019**, *9*, 1574. DOI
248. Suriyakumar, S.; Stephan, A. M.; Angulakshmi, N.; Hassan, M. H.; Alkordi, M. H. Metal-organic framework@SiO_2 as permselective separator for lithium-sulfur batteries. *J. Mater. Chem. A.* **2018**, *6*, 14623-32. DOI
249. Bai, S.; Zhu, K.; Wu, S.; et al. A long-life lithium-sulphur battery by integrating zinc-organic framework based separator. *J. Mater. Chem. A.* **2016**, *4*, 16812-7. DOI
250. Zhou, C.; He, Q.; Li, Z.; et al. A robust electrospun separator modified with in situ grown metal-organic frameworks for lithium-sulfur batteries. *Chem. Eng. J.* **2020**, *395*, 124979. DOI
251. Huang, J. Q.; Zhuang, T. Z.; Zhang, Q.; Peng, H. J.; Chen, C. M.; Wei, F. Permselective graphene oxide membrane for highly stable and anti-self-discharge lithium-sulfur batteries. *ACS. Nano.* **2015**, *9*, 3002-11. DOI
252. Lammert, M.; Glißmann, C.; Reinsch, H.; Stock, N. Synthesis and characterization of new Ce(IV)-MOFs exhibiting various framework topologies. *Cryst. Growth. Des.* **2017**, *17*, 1125-31. DOI
253. Lee, D. H.; Ahn, J. H.; Park, M.; Eftekhari, A.; Kim, D. Metal-organic framework/carbon nanotube-coated polyethylene separator for improving the cycling performance of lithium-sulfur cells. *Electrochim. Acta.* **2018**, *283*, 1291-9. DOI
254. Jiang, G.; Zheng, N.; Chen, X.; et al. In-situ decoration of MOF-derived carbon on nitrogen-doped ultrathin MXene nanosheets to multifunctionalize separators for stable Li-S batteries. *Chem. Eng. J.* **2019**, *373*, 1309-18. DOI
255. Wang, B.; Liu, J.; Mao, C.; et al. A MOF-gel based separator for suppressing redox mediator shuttling in Li-O_2 batteries. *Small* **2024**, *20*, 2401231. DOI
256. Guang, Z.; Huang, Y.; Chen, C.; Liu, X.; Xu, Z.; Dou, W. Engineering a light-weight, thin and dual-functional interlayer as "polysulfides sieve" capable of synergistic adsorption for high-performance lithium-sulfur batteries. *Chem. Eng. J.* **2020**, *383*, 123163. DOI
257. Li, B.; Pan, Y.; Luo, B.; et al. MOF-derived $NiCo_2S_4$@C as a separator modification material for high-performance lithium-sulfur batteries. *Electrochim. Acta.* **2020**, *344*, 135811. DOI
258. Li, W.; Ye, Y.; Qian, J.; et al. Oxygenated nitrogen-doped microporous nanocarbon as a permselective interlayer for ultrastable lithium-sulfur batteries. *ChemElectroChem* **2019**, *6*, 1094-100. DOI
259. Cai, J.; Song, Y.; Chen, X.; et al. MOF-derived conductive carbon nitrides for separator-modified Li-S batteries and flexible supercapacitors. *J. Mater. Chem. A.* **2020**, *8*, 1757-66. DOI